Amsterdam UMC
Universitair Medische Centra

TU Delft
Delft University of Technology

Thesis

Foetal Imaging: Optimising Lugol's Solution Staining for CT Scanning

Tessa de Vries (4749928)
MSc Biomedical Engineering, Medical Physics
Date of defence: 2nd of July 2021

Amsterdam UMC, location AMC
Meibergdreef 9, 1105 AZ, Amsterdam
Supervision: Yousif Dawood

Technische Universiteit Delft, Faculty 3mE
Mekelweg 2, 2628 CD, Delft
Supervision: Marlies Goorden

Abstract

Biomedical researchers and clinicians are interested in (ab)normal foetal development because it can aid in better understanding human anatomy. To capture this foetal development non-destructive three dimensional (3D) imaging techniques like computed tomography (CT) are used. Visualising foetuses remains a challenge however, as foetuses consist mostly of soft-tissue. Visualisation of soft-tissue with CT scans is difficult because X-rays easily pass through. This consequently results into images with low contrast. Therefore, improving contrast is artificially gained by using chemical compounds called stains. The most effective stain is considered to be Lugol's solution. A downside of using Lugol's solution is that the staining process causes extensive soft-tissue shrinkage which is detrimental for morphological analysis. The mechanism of Lugol-induced shrinkage is largely unknown. Some research suggest it is due to an osmotic imbalance between tissue and solution, while others point towards acidification of Lugol's solution. The goal of this study is to develop an optimum (buffered) Lugol's solution staining protocol for post-mortem human foetal CT imaging to diminish soft-tissue shrinkage and achieve homogeneous staining. Several variables in the protocol are taken into account such as staining solution concentration, staining time and specimen size. To develop this protocol, multiple tests and measurements (pH, osmolarity, optical density, weight and CT scans) were performed on pork liver samples and two post-mortem human foetuses to monitor acidification of the staining solution, staining progress and staining intensity, while applying two distinct methods: the AMC- and Arthurs method. The main difference between these methods is that the AMC method fixates tissue well before staining (conventional method), while Arthurs method uses a mixture of a fixative and stain simultaneously on fresh tissue. The research suggests that Arthurs method seems best. Even though, both methods led to a homogeneous staining, the AMC method resulted in an average shrinkage of 4.82%, while Arthurs method resulted in a shrinkage of only 1.08%. In addition, Arthurs method leads to a shorter staining protocol.

Keywords: *3D medical imaging, anatomy, computed tomography, ethics, foetal imaging, foetus, Lugol's solution, soft-tissue staining, staining protocol.*

Nomenclature

3D	Three Dimensional
AMC	Academisch Medisch Centrum
CB	Citrate Buffer
CT	Computed Tomography
DiceCT	Diffusible Iodine Contrast Enhanced Computed Tomography
F	Formalin
FB	Formalin Buffer
HU	Hounsfield Unit
L	Lugol's solution
METC	Medical Ethical Review Committee
MRI	Magnetic Resonance Imaging
OD	Optical Density
PIF	Patient Information Form
PBS	Phosphate Buffered Saline
PFA	Paraformaldehyde
SB	Sörensen's Buffer
TOP	Termination of Pregnancy
w/v	weight/volume

Preface

This document covers research on "Foetal Imaging: Optimising Lugol's Solution Staining for CT Scanning", performed at the AmsterdamUMC (location AMC), in which I was engaged from January to July 2021. This thesis has been written to obtain the degree of *Master of Science* at the Delft University of Technology, Faculty 3mE.

Thesis committee:

Yousif Dawood
Amsterdam UMC / Department of Obstertics and Gynaecology | Department of Medical Biology

Maurice van den Hoff
Amsterdam UMC/ Department Medical Biology

Marlies Goorden
TU Delft Applied Sciences/ RST

Robin de Kruijff
TU Delft Applied Sciences/ RST

An electronic version of this thesis is available at http://repository.tudelft.nl/.

Special thanks to:

Yousif Dawood	For supervising my graduation project, asking the right questions which made me think, frequent meetings and giving feedback on my work.
Maurice van den Hoff	For guiding the Foetal Imaging project, brainstorming during our frequent meetings and hiring me.
Jaco Hagoort	For helping me with the use of AMIRA software and frequent meetings.
Quinn Gunst	For the lab tour when I started at the AMC and always being open for questions.
Gustav Strijkers	For performing MRI scans on short notice.
Marlies Goorden	For being my TU Delft supervisor, taking care of the paperwork and making me feel that I could say and ask anything.
Samantha Copeland	For the brainstorming session about the ethical dilemmas regarding foetal donation.
Yorben Blok	For "pre-reading" my text.

Tessa de Vries – 25th of June 2021

Contents

1. Introduction

Biomedical researchers and clinicians have been interested for a long time in (ab)normal foetal development to better understand human anatomy. Traditionally, the combination of histological sectioning and confocal microscopy was used to create three dimensional (3D) images. [1] However, besides that these traditional techniques are destructive, further downsides are: possible tissue distortion, limited resolution and time consuming image reconstruction. [2] Since 2009, non-destructive 3D imaging techniques like computed tomography (CT) are used to visualise foetal development in high resolution 3D images and relative short scanning times. [3] However, visualising foetuses is a challenge because foetuses consist mostly of soft-tissue. Soft-tissue visualisation with CT is difficult because X-rays easily pass through soft-tissue (less dense tissue) instead of being absorbed. If X-rays are not absorbed it results in images with low contrast, which makes differentiating between soft-tissues difficult. To better distinguish soft-tissue with CT imaging, solutions of chemical compounds that contain elements with high atomic numbers are used. These high atomic numbers cause the density to increase artificially and results into more X-ray absorption which consequently leads to higher contrast images and better visualisation of soft-tissues.

Many different chemical compounds, also called "stains", are available to enable soft-tissue visualisation for CT scanning. The most effective stain is considered to be potassium triiodide (I_2KI) solution, also known as Lugol's solution. This is because of its ease of handling, cost-effectiveness and differential affinities for major types of soft-tissue. [4]–[6] A downside of using Lugol's solution is that the staining process causes extensive soft-tissue shrinkage, which also varies across tissue types. [2], [7], [8] Literature suggests that tissue shrinkage can be caused by two different routes. One of which is due to an osmotic imbalance between tissue and solution [2], [8]–[10]. However, using different tonicities of the solution does not seem to prevent tissue shrinkage. [11] Therefore, an osmotic imbalance does not seem to be the sole mechanism. [2], [8], [12] Other experiments show a strong correlation between tissue shrinkage and acidification of Lugol's solution [11], but this correlation has received limited further attention in the research. Evaluating the correlation between acidification of Lugol's solution and tissue shrinkage is important because tissue deformation is detrimental for morphological analysis. For example, in clinical or forensic cases tissue shrinkage can result in a false diagnostic conclusions. Therefore, this study researches acidification of Lugol's solution to further develop an optimum staining protocol that diminishes tissue shrinkage while achieving a homogeneous staining for proper imaging.

The goal of the research is formulated in the following main research question: "*What is the optimum (buffered) Lugol's solution staining protocol for post-mortem human foetal CT imaging to achieve homogeneous staining and diminish soft-tissue shrinkage, while taking into account staining solution concentration, staining time and specimen size?*" To answer this question it is split up into two sub-questions:

1. Can shrinkage artefacts be diminished by using buffered Lugol's solution in comparison to normal Lugol's solution?
2. What is the difference in pH stability over time comparing normal Lugol's solution, Sörensen's buffered Lugol's solution and citrate buffered Lugol's solution?

To answer the research questions, multiple tests and measurements (pH, osmolarity, optical density, and weight) and CT scans were performed on soft-tissues. Soft-tissues used were pork liver samples and post-mortem human foetuses. The tests and measurements were applied via two distinct methods: the conventional AMC method and Arthurs method. As noted in the research questions, other factors that will be considered as to the success of an optimum staining protocol are specimen size, staining solution concentration and staining time. [13]

This study starts with background information (*Chapter 2*) about Lugol-induced tissue shrinkage, buffers, staining protocol steps and the importance of homogeneous staining. *Chapter 3* is about the ethics regarding foetal donation. In *Chapter 4*, the applied methods (AMC and Arthurs) and the materials/preparations are described. The results can be found in *Chapter 5*, followed by a discussion in *Chapter 6*. Finally, the conclusion is given in *Chapter 7* were also further research is proposed.

2. Background Information

This chapter provides background information about Lugol-induced tissue shrinkage, buffers, staining protocol steps, the AMC- and Arthurs method and the importance of homogeneous staining.

2.1 Lugol-Induced Tissue Shrinkage and Buffers

In this study, Lugol's solution (I_2KI) is chosen as staining solution because it is considered in previous research as the best option for staining soft-tissues. Advantages are its ease of handling, reversibility, cost-effectiveness and differential affinities for major types of soft-tissue (see **Appendix I – Literature Study** for more information). Lugol's solution is a mixture of one part iodine (I_2) and two parts potassium iodide (KI) in water. Due to the popularity of Lugol's solution, it is the most commonly used staining solution and literature is generally available. [4]–[6] A downside of using Lugol's solution is that the staining process causes extensive soft-tissue shrinkage, which also varies across tissue types. [2], [7], [8] Diminishing (or even preventing) tissue shrinkage in foetal 3D imaging is important, because shrinkage of soft-tissues can result into: distorted/less realistic 3D images and false diagnoses.

The mechanism behind Lugol-induced tissue shrinkage is still largely unknown. Multiple researchers state that Lugol-induced tissue shrinkage is due to an osmotic imbalance between tissue and solution. [2], [8]–[10] An osmotic balance ensures (by diffusion of water or solutes) that optimal concentrations are maintained in cells, body tissues and fluids. [14] Dawood et al. found that using different tonicities[1] of Lugol's solution did not prevent tissue shrinkage. For example, hypertonic solutions can cause tissue shrinkage due to the extraction of water from the tissue. [2] Because the different tonicities did not prevent tissue shrinkage, the osmotic imbalance demonstrates not to be the sole mechanism behind tissue shrinkage. During these experiments, Dawood et al. did see a significant pH decrease over time for all solutions tested, except for the control samples. Therefore, it is suggested that acidification of Lugol's solution over time could be the main cause of tissue shrinkage instead of changes in osmotic balance. [11]

Following the research from Dawood et al. the hypothesis is that tissue shrinkage could be diminished by preventing acidification of Lugol's solution. Acidification of Lugol's solution can be prevented by adding a buffer to Lugol's staining solution. A buffer is used to keep the pH stable upon adding acidic or basic components. The buffer ensures that the chemical reaction rates of forward and reverse reactions are the same to keep the pH stable. [15] The amount of acid or base that can be neutralized by the buffer to keep the pH stable is called the buffer capacity or buffer strength (indicated with for example 1x). [16] [17] In short, the buffer is used to keep the Lugol's solution in a neutral pH range, thereby avoiding acidification and prevent tissue shrinkage. Two types of buffers were included in this study: i) Sörensen's buffered Lugol's solution and ii) citrate buffered Lugol's solution.

In this study the osmolarity (amount of solutes) in the Lugol's solution, is described as a weight/volume (w/v) concentration. 15% w/v Lugol's solution (which is also referred to as 100% Lugol's solution in other studies since higher concentrations are normally not used) has an I_2 concentration of 986 $mmol/L$

[1] Tonicity is the relative concentration of solutes dissolved in a solution that determines the direction and amount of diffusion. There are three types of tonicities: isotonic, hypotonic and hypertonic. Cells immersed in isotonic solutions remain stable in volume, cells immersed in hypotonic solutions increase in volume and cells immersed in hypertonic solutions decrease in volume. The amount of increase/decrease of volume has to do with the net flow of water into or out of the cell. [36]

and an osmolarity of 1204 $mOsm/L$. [2] Lower concentrations of Lugol's solution can be made by diluting with water as long as the researchers specify the water source. [4]

2.2 Staining Protocol

In general, a staining protocol provides information about: fixation (if applicable), staining and imaging. Below each element is addressed in turn.

Fixation

A fixation solution (fixative) is used to: i) halt tissue autolysis and ii) ensure tissue integrity [7] [18]. This is important because studying a foetus for foetal imaging can take up to multiple days. Gignac et al. recommend to prepare for fixation the "freshest" possible tissues in order to maximize the quality of the specimens sampled. [4] For choosing the fixative, personal preference, costs and availability are taken into account.

In this study, two types of staining protocols were applied: the "AMC method" (conventional protocol developed at the AmsterdamUMC) and a more time efficient protocol "Arthurs method" (protocol developed by Arthurs et al. [18]). Performing the AMC method, soft-tissue samples are fixed first. The fixative used is 4% w/v paraformaldehyde (PFA) in Phosphate Buffered Saline (PBS, 10mM H_2NaPO_4/HNa_2PO_4, 150 mM NaCl, pH 7.4) at 4ºC. After fixation, the samples are stored in 0.2% PFA in PBS in 4ºC until usage.

Although it is common to first fix the sample (to halt tissue autolysis and ensure tissue integrity) and stain later, Arthurs et al. describe a different method. [18] The main difference compared to the AMC method is that Arthurs et al. do not fixate before staining, but use a mixture of a formalin (the fixative) and stain simultaneously during the staining process.

Staining

As aforementioned, soft-tissue provides less contrast in CT imaging because X-rays pass easily through low density structures compared to more dense tissues. The low contrast on CT images makes it difficult to differentiate between soft-tissues. The problem is that the difference in attenuation coefficients (μ) is (too) small to distinguish between soft-tissues. To allow a bigger difference in attenuation coefficient – and consequently increase the contrast in the image to be able to distinguish between different soft-tissues – it is necessary to use a staining solution. [6][19] Stains used are high density fluids with a high atomic number to artificially achieve higher levels of X-ray attenuation for soft-tissue.

An example of a CT image of a post-mortem foetus without and with increasing the attenuation coefficients by using Lugol's solution staining can be seen in *Figure 1*.

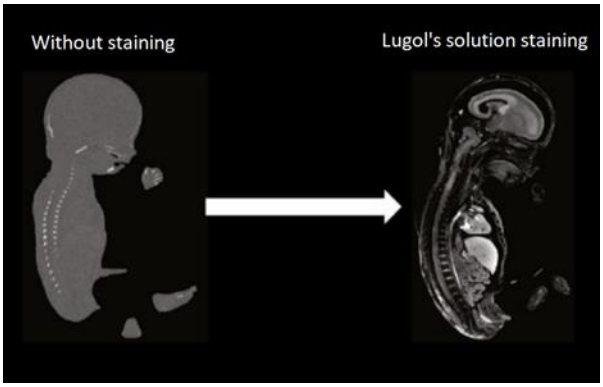

Figure 1 *µCT images of a human post-mortem foetus.* ***Left****: without staining.* ***Right****: with Lugol's solution staining. This illustrates the increase of attenuation coefficient and therefore soft-tissue visualization due to Lugol's solution staining.* [7]

A CT scanner reconstructs the value of the attenuation coefficient at each pixel within a cross section and expresses this as Hounsfield Units (HU) (as shown in *Formula 1*):

$$HU = 1000 \cdot \frac{\mu - \mu_{water}}{\mu_{water}} \quad \textbf{(1)}$$

For water, $HU = 0$. In air, $\mu = 0$ and $HU = -1000$. Soft-tissues, for example liver, show values of $HU \approx 70$. More dense tissues, for example bone, have high HU values of ≈ 1000. If stains are used, the CT values can even go up or beyond values of $HU \approx 3000$. [20]
In this study, Lugol's solution is used as staining solution. The HU value of Lugol's solution differs with the applied staining concentration (% w/v). In *Figure 2*, a graph is presented of a diluted Lugol's solution series. The concentration of Lugol's solution and corresponding HU values are respectively: 3.85 & 843, 5.33 & 1126, 7.57 & 1645 and 16.15 & 3068. In addition, the staining intensity also depends on the binding affinity of Lugol's solution to soft-tissue. Lugol's solution has a binding preference to a.o. haemoglobin, glycogen, carbohydrates and lipids. [8], [21] For example, after staining with Lugol's solution, liver tissue gets better visualisation as the abundantly present haemoglobin easily binds Lugol's solution.

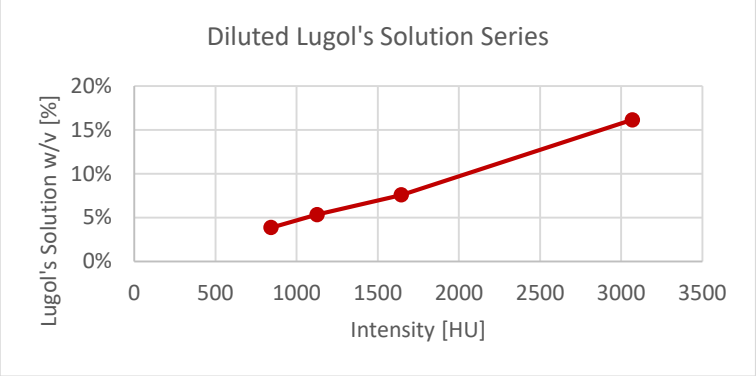

Figure 2 *Diluted Lugol's solution series. Staining concentration (% w/v) of Lugol's solution plotted against the CT values (intensity) in HU.*

Both Arthurs method and the AMC method use the same stain: Lugol's solution. The AMC method uses Lugol's solution of 3.75% w/v Lugol's solution, Arthurs Method uses a 15% w/v Lugol's solution. However, Arthurs et al. subsequently dilute the Lugol's solution 1:1 with 10% w/v formalin. This mixture results in a 7.5% Lugol-Formalin (LF) solution which stains and fixates simultaneously. [18] For both methods the sample(s) can be positioned onto a horizontal shaker (or belly dancer) to allow a more rapid exchange of solutes during the staining process.

Imaging
CT scanning such as "Diffusible Iodine Contrast Enhanced Computed Tomography" (diceCT) is frequently used in morphological research since it can be an addition, or even a replacement, for conventional autopsy. [7] For the avoidance of doubt, DiceCT means both staining (with a staining solution that contains iodine, like Lugol's solution) and CT scanning. DiceCT therefore enables the study of development and anatomy of internal structures, including soft-tissues, without being destructive. Besides the high-resolution images and its non-destructive character, diceCT is much faster than classic histology, taking only minutes rather than days.
In this study, a SOMATOM clinical CT scanner (Siemens Healthineers AG, Erlangen, Germany) with a resolution of 0.2 mm x 0.2 mm x 0.1 mm is used. CT scans were made with the pre-programmed setting "RESEARCH-1414_Lugol_test(Adult)" – developed by G. Strijkers – in which the parameters were set to a voltage of 150 kV and current of 200 Eff. mAs. These scan settings were based on experiences of G. Strijkers and findings of Y. Dawood and not further elaborated on in their research. Additional information about CT can be found in **Appendix I – Literature Study**.
After scanning, the obtained DICOM-files are processed in AMIRA version 2020.2 (Thermo Fisher 271 Scientific, United States) to estimate total volume, evaluate staining progress and staining intensity.

As a side note, immersion in Lugol's solution to achieve better CT images reduces the accuracy of Magnetic Resonance Imaging (MRI). Therefore if complementary imaging tests with MRI are used as reference, they must be completed prior to staining the tissue as with diceCT. At the AMC, an MRI scan (7T MRI; MR Solutions, Guildford, UK) is made as a starting reference for the volume of the entire foetus including its organs. This is preferred as an MRI scan better shows the anatomical detail of a foetus at an early developmental stage without staining.

2.3 Importance of Homogeneous Staining

Staining uptake in soft-tissue happens over time by relying on passive diffusion. Diffusion, or spreading, is the movement of particles from a region of higher concentration (many solutes in the staining solution) to a region of lower concentration (the unstained sample) across the plasma membrane. This membrane (phospholipid bilayer) is a barrier, present around all cells. The difference in solute concentration between each side of the membrane is the driving force for passive diffusion and requires no energy. Over time (during the staining process), the concentration is equalized (see *Figure 3).* [22][23] Besides staining time, complete staining of the sample also depends on the specimen size and used staining solution concentration. [2], [7]

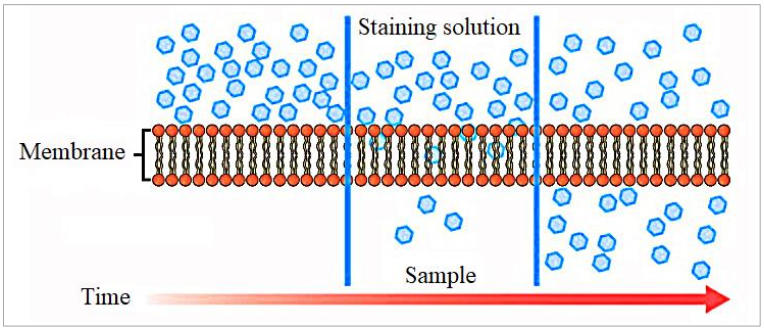

Figure 3 *Passive diffusion illustrated. Over time, solutes will move from high concentration (the staining solution) to a low concentration (the sample) until the concentration on both sides of the membrane is equal.* [23]

For staining soft-tissue in CT imaging, it is required that the staining solution is homogeneously distributed over the sample. If the staining is not homogeneously distributed (concentration is not equalized throughout the sample), there is a chance of under- or overstaining. Both under- and overstaining can lead to undesirable CT imaging results because in both cases contrast issues occur which consequently can result into less realistic 3D images and wrong diagnoses. To avoid under- or overstaining, it of course important to adjust staining times based on specimen size. [4]

Under-staining mostly happens when the sample is prematurely removed from the staining solution. As a consequence, the staining will be incomplete and parts of the sample (mostly the inner parts) will retain their low contrast properties when CT imaged. An example of under-staining, also called incomplete staining, can be seen in *Figure 4*, provided by Dawood et al. [13]

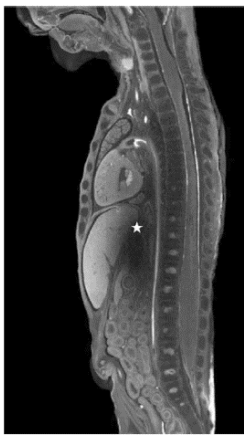

Figure 4 *µCT image of a Lugol's solution stained foetus. 72 hours staining with 3.75% Lugol's solution result in understaining (star). [7]*

An incomplete staining process can also be identified by the intensity line profile of a stained sample not having a relatively flat line (a plateau). *Figure 5* shows an example of intensity line profiles and CT images for 0, 13 and 58 h. staining time (time that the sample is immersed in the staining solution). The intensity line profile visualises the staining progress and staining intensity in HU values (y-axis) over the sample distance in mm (x-axis) towards the centre. The staining progress is visible by a flatter line (the plateau), the staining intensity is visible by the overall height of the plateau. As is visible, the graph also shows a plateau for 0 h. staining. This is the obvious result of a sample with no staining progress (staining progress is non-existent) and a low staining intensity (all HU values are derived from the unstained sample). The CT images presented below show an increase in contrast due to staining.

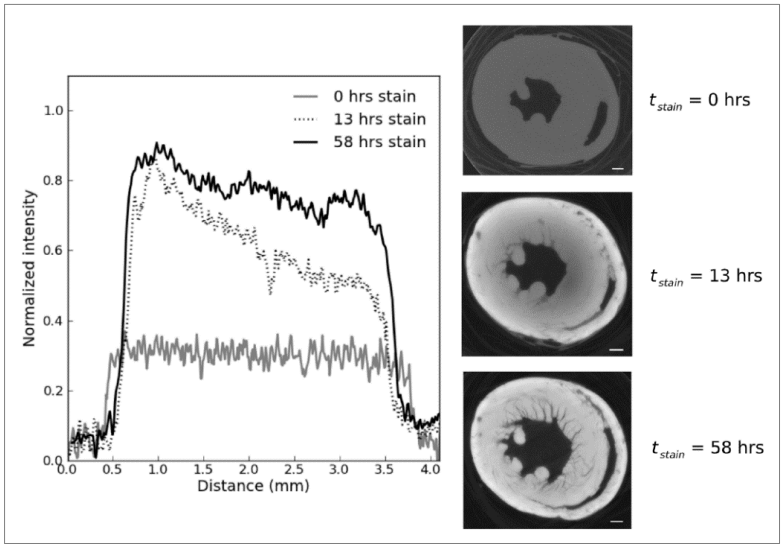

Figure 5 *Intensity line profiles and CT images for 0, 13 and 58 h. staining time. This is an example of a cross section of the ventricular wall (heart) of an adult mouse. Images are provided by Butters et al.* [24]

With longer staining times the number of voxels[2] with a large attenuation coefficient, corresponding to a high amount of stain accumulation, increases. More information on attenuation coefficients can be found in **Appendix I – Literature Study**. In short, as the staining time increases and passive diffusion reaches equilibrium, the intensity line across the tissue becomes higher and flatter which creates a plateau in the graph. A flatter line means a more uniform intensity, which is expected for homogeneously stained tissue. [24], [25] A consequence of incomplete staining is that the use of automated methods for (organ) segmentation is difficult, as these methods often rely on each distinct region having consistent intensity. [24]

Over-staining can result in sample deformation and tissue shrinkage. [24], [26] Moreover, analysing the overstained image can be difficult due to the staining intensity reaching or exceeding the maximum range of the CT scanner. In that case, all overstained soft-tissue will have a high attenuation which results in similar absorption of X-rays and subsequent into low contrast images (as with unstained soft-tissue). The intensity line across the tissue will then be a very flat and high plateau, meaning that the "real" intensity is probably out of the range of the CT scanner.
Over-staining becomes an issue more easily if a high concentration of Lugol's solution is used (10% w/v or higher) as high concentrations more quickly lead to loss of tissue differentiation (X-ray attenuation too high) during CT scanning [4] and/or soft-tissue shrinkage [8], [27].

2.4 Schematic Overview

This chapter contains lots of information about low contrast CT imaging of soft-tissues, X-ray absorption, artificially achieving higher CT imaging contrast, the importance of homogeneous staining and preventing tissue shrinkage to finally result in better CT imaging results to achieve more realistic

[2] 3D equivalent of pixels

3D visualisations and better diagnosis. All these problems, their solutions and the study goals are visualised in a schematic overview which can function as a reference while reading this report (see *Figure 6*).

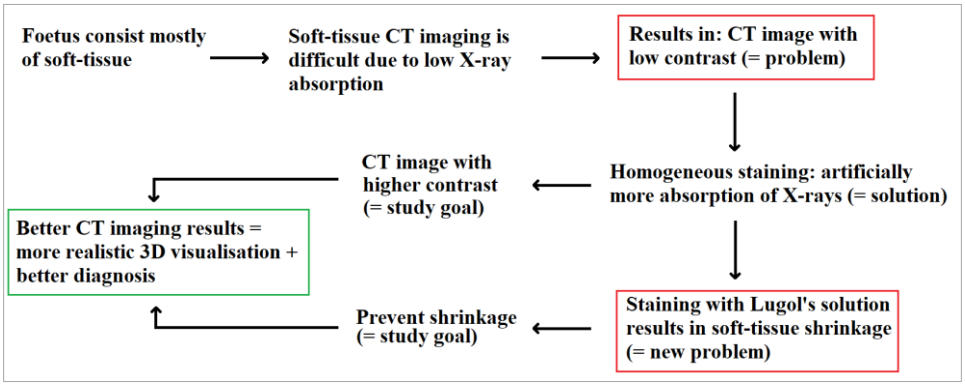

Figure 6 *Schematic overview of low contrast CT images and how to solve this with staining. Staining with Lugol's solution results into tissue shrinkage. By preventing tissue shrinkage and applying staining, a better CT image can be obtained which results into more realistic 3D visualisations and a better diagnosis.*

3. Ethics regarding Foetal Donation

The Netherlands is uniquely positioned internationally for foetal imaging because there is an option to donate a foetus to science after a stillbirth, miscarriage or abortion (termination of a pregnancy, abbreviated as: TOP) instead of opting for the usual collective cremation. Since the AMC only started scientific research on foetal imaging back in 2018, there are not many scientific sources to consult or to substantiate the ethics around foetal donation (and imaging). To fill this gap, future projects related to foetal imaging could incorporate an ethics-oriented investigation. This study aims to make a start.

Normally, anyone who wishes to conduct in scientific research that requires the participation of test subjects is required to visit a recognised Medical Ethical Review Committee (Medisch Etische Toetsings Commissie, or METC). The METC AMC is the recognized committee of the AMC. Participants undergo a medical-ethical assessment which is part of the "Medical Research Involving Human Subjects Act (Wet medisch-wetenschappelijk onderzoek met mensen)". [28] The issue however, is that this study focusses on foetuses. Foetuses cannot indicate that they want to participate in scientific research and therefore the parents have to make the decision.

To participate in foetal imaging research, the AMC has set up an informed consent procedure in such a way that the parents must first have made a final decision about termination of the pregnancy. After that, the AMC notifies the parents about the foetal imaging research and that they have the option to donate their foetus. Notifying the parents is performed via an informed consent procedure. During this procedure, the parents receive a Patient Information Form (PIF). The PIF contains information about the research (purpose-, location- and duration of the study), a scientific research consent form and a withdrawal form. Since the whole procedure has to be formally confirmed, the scientific research consent form must be signed by the parents if they want their foetus to participate. Depending on the diagnosis of the foetus (normal/healthy or a deviation) there are different PIFs. An example of a PIF to study Down Syndrome can be found in **Appendix II – Ethics: Patient Information Form (Dutch Only)**.

After the parents have received the PIF, they are given some time to consider the donation. The parents face a though ethical dilemma at this stage. For example, many parents cope with questions about why their child died but are not pleased with a conventional destructive autopsy. In this case, a virtual autopsy with the use of 3D imaging may provide answers about why the pregnancy ended and if there is a possibility whether it might happen again in the future. Another, perhaps comforting example is that sometimes parents let the AMC know that by donating their foetus to science, they can cope with the loss of their child in a better way. [29] Since the parents likely have an emotional attachment to the

foetus, it might be reassuring to know that the foetus is going to contribute to science and that the parents know exactly how. Another interesting ethical concern for the parents or family could be bodily integrity after death which may obviously vary between cultures.

If the parents decide to donate their foetus for research, the foetus will serve science in two ways. First, the AMC is building a so-called biobank with different tissues (the Dutch Foetal Biobank). In this biobank, collections of body materials are established and stored for scientific research. Secondly, the imaging will be used to add information to the Atlas of Embryology (which was presented in the journal Science in 2016 – www.3datlasofhumanembryology.com). [1] The goal of this atlas is to present in unprecedented detail (rotatable 3D images) how the foetus and different organs develop during pregnancy (0 – 24 weeks).

Upon receipt of the foetus by the researchers, the foetus is completely anonymized. This means that the foetus cannot be traced back to the parents after donation.

4. Materials & Methods

This chapter describes what personal protective equipment one must use, how to prepare solutions, what types of solution measurements were performed, which (buffered) Lugol's solutions were made as a staining solution, which CT scanner was used and what software measurements were performed on the DICOM-data.

4.1 Personal Protective Equipment

During the preparations of the (staining) solutions in the lab, as well as while working with the stained soft-tissue samples, hazardous substances are used. Lugol's solution contains I_2 which is toxic if taken orally and can cause skin irritation or even tissue damage. While mixing (Lugol's) solutions together, it is therefore necessary to work under a fume hood to limit exposure to hazardous fumes. Furthermore, since acidic solutions are used, it is important to wear gloves and a lab coat with long sleeves at all times. Hazardous substances can be recognized by various symbols (warning signs).

4.2 Preparations

Before one of the two methods (AMC or Arthurs) can be performed, the so called "stock solution" preparations are required. This means weighing out an appropriate portion of a solid or measuring out a volume of a liquid. In this study, three different stock solutions are prepared and used next to Lugol's solution, namely: Sörensen's buffer, citrate buffer and formalin. All solutions are mixed in glass Erlenmeyers and magnetically stirred. If the stock solution is finished, it can be stored in a glass bottle to use later on.

15% w/v Lugol Solution

The easiest way to prepare a 15% w/v Lugol's solution is by mixing together 5 g. I_2, 10 g. KI and bring it to and end volume of 100 mL with Milli-Q water (purified tap water). In this study, I_2 and KI 99%+ from Fischer Scientific are used. Solid I_2 is grounded by a mortar and pestle for quicker dissolvent. KI is already quickly soluble by itself. The powder(s) should be dissolved in the water in a couple of minutes. This results in a dark brown mixture called Lugol's solution. Lastly, Lugol's solution should be stored in the dark (aluminum foil can be used to wrap around the bottle) because it is light sensitive. If other amounts or concentrations of Lugol's solution are required, combine and dilute appropriately (with Milli-Q water).

Sörensen's- and Citrate-Buffer

Sörensen's Buffer (SB) and citrate Buffer (CB) are considered the easiest to make as 2x buffer-stock solutions because after combining and diluting appropriately you end up with a 1x buffer (which is the strongest buffer capacity used in this study).

SB consists out of Na_2HPO_4 and KH_2PO_4, while CB consists out of citric acid and Na_2HPO_4. In this study it was considered most convenient to make 266 mM solutions (which results into a 2x buffer) for both SB and CB. For SB, start with making two solutions: i) 71.52 g. $Na_2HPO_4.5H_2O$ in 1 L bidistilled water and ii) 18.16 g. KH_2PO_4 in 1 L bidistilled water respectively. To make a 2x SB, combine 71.5 mL Na_2HPO_4 with 28.5 mL KH_2PO_4 for a pH of 7.20.

For CB, a 2x buffer was made by mixing together different volumes (x mL) of 0.2 M-citric acid and (y mL) of 0.4-Na_2HPO_4. By combining different volumes for x and y, three different CBs were made with different pH values (see *Table 1* for an overview of volume for x and y and the resulting pH value). More pH values for CB can be found in **Appendix III – Buffers**.

Table 1 *Citrate-buffer pH values.*

pH	*x mL* 0.2*M*-citric acid	*y mL* 0.4-Na2HPO4
3.00	79.45	20.55
5.00	48.50	51.50
7.00	17.65	82.35

Formalin

Formalin fixative is an essential solution to perform the Arthurs method. Mix together 45 g. sodium chloride (NaCl) with 500 mL 40% w/v formaldehyde and 4500 mL water to get a total volume of 5000 mL 10% w/v formal saline (formalin) solution. [18] This mixture results into a 4% formaldehyde solution because it is diluted 1:10, but it is referred to as 10% w/v formalin during this study. Combine and dilute appropriately, depending on how much solution is required.

Fill in Sheets

Preparing fill in sheets (and printing them) to write down measurement results is very practical. An example of a fill in sheet can be found in **Appendix IV – Example Fill in Sheet**.

4.3 Solution Measurements

As noted before, research suggests that tissue shrinkage is due to an osmotic imbalance between tissue and solution [8]–[10]. However, pilot experiments pointed to the role of acidification of Lugol's solution rather than osmotic imbalance. [11] Although acidification of Lugol's solution was noted before, its relation with tissue shrinkage has not been properly evaluated. In this study, the relation between tissue shrinkage, osmolarity and acidification of the solution during staining are therefore systematically analysed. To monitor this relation, pH values, osmolarity and optical density of the staining solutions were measured at predefined time points before and during all tests.

pH Measurements

pH measurements were performed to closely monitor the acidification of the solutions and its correlation with tissue shrinkage. pH was measured using a Consort P901 261 Electrochemical analyzer (Consort bvba, Turnhout, Belgium). To measure the pH of a solution, take the electrode from the KCl solution (3 – 4 M) and rinse it (after every measurement) with distilled water. The equipment should be calibrated before use. The calibration is performed with pH values of 4.00, 7.00 and 9.18. After calibration, immerse the electrode in the samples and read the pH value from the display. If all measurements are performed, rinse the electrode and store it in the KCl solution. Storing the electrode in KCl is important because the electrode is active and stable only after wetting. [30]

Optical Density (OD) Measurements

OD measurements are performed to quantify the remaining concentration of triiodide (I^{3-})in the staining solution. This is because over time, the triiodide in Lugol's solution binds to soft-tissue. This binding results into a decrease of triiodide in the staining solution. Visually, one can see the dark brown mixture of Lugol's solution being absorbed by the sample which leads to a darker sample and more transparent Lugol's solution. This change in the colour of Lugol's solution is also the basis on which OD

measurements are conducted. OD is measured using the Thermo Scientific NanoDrop™ 1000 Spectrophotometer (Thermo Fisher Scientific, United States). It measures the OD of 1 μL samples with high accuracy and reproducibility. With the sampling arm open, 1 μL droplet is pipetted onto the end of a fibre optic cable (the receiving fibre). A second fibre optic cable (the source fibre) is then brought into contact by closing the sampling arm with the droplet as a bridge of gap between the fibre optic ends. A pulsed xenon flash lamp provides the light source and a spectrometer is used to analyse the light passing through the liquid. The less light passes through, the more dense the liquid is and vice versa. It is important to start with a blanc measurement to calibrate (with 1 μL of distilled water) and wipe the 1 μL droplet from the pedestals upon completion of each sample measurement. The instrument is controlled by PC based software with function UV-Vis at 550 nm. The data is logged in an archive file. [31]

To express the percentage w/v of Lugol's solution that is present in the staining solution from the OD measurement, a calibration line is used. In *Figure 7,* multiple OD measurement results are plotted against a diluted Lugol's solution concentration series (approximately 0.47%, 1.88%, 3.75% and 7.5% w/v). From these results, a linear trend line ($y = 154.63x - 46.639$) is plotted. This trend line can be expressed as *Formula 2,* to determine the percentage w/v of Lugol's solution in the staining solution.

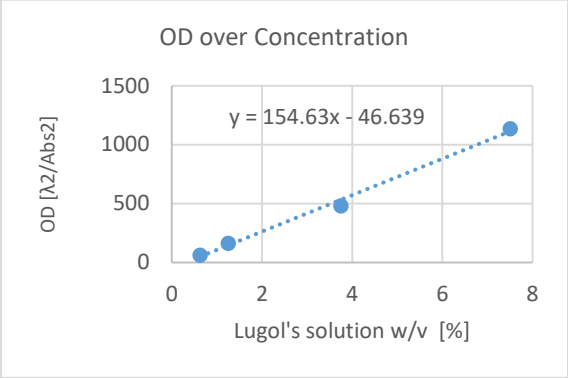

Figure 7 *Linear trend line: OD plotted against Lugol's solution concentrations.*

Formula 2:

$$Lugol\ w/v\ [\%] = \frac{OD_{550} * 1000 + 46.639}{154.63} \quad \textbf{(2)}$$

Where OD_{550} refers to the Nanodrop OD measurement result performed with function UV-VIS at 550 nm.

Osmolarity Measurements

As a double/safety check, osmolarity measurements were performed to see if next to acidification there might be any correlation between osmotic imbalance and tissue shrinkage. Osmolarity was measured using a Salmenkipp OSMOMAT 030 cryoscopic osmometer which is an automatic osmometer that measures the freezing point depression with a measurement tip to determine the total osmolarity of aqueous solutions. The calibration of the osmometer happens automatically. In this experiment 50 μL from the solutions is pipetted into disposable Eppendorf tubes. The tubes are positioned inside the osmometer. The measurement starts automatically by closing the lid. [32] It is advisable to keep a piece of paper towel within reach to clean excess (frozen) solution from the measurement tip before putting the next Eppendorf tube into position to allow more precise osmolarity measurements.

4.4 Tests on Different (Lugol's) Solutions

Prior to staining the actual foetuses, four tests were performed on solutions and/or on pork liver samples. With the conventional AMC method, as a first test, 25 different solutions[3] were made to study pH stability, osmolarity and OD after mixing Lugol's solution together with buffers. The buffers, SB and CB, were used to keep the pH values steady at 7.00, 5.00 and 3.00. For convenience, the notation of the different solutions is indicated with letters and numbers. For example: SB7-1, where the letters represent the type of solution used (SB), the first number refers to the initial pH value (pH 7) and the last number refers to the buffer strength (1x). Further explanation of the abbreviations can be found in **Appendix V – Solutions without Tissue**.

[3]S1, S0.5, S0.25, SB7-1, SB7-0.5, SB7-0.25, C7-1, C7-0.5, C7-0.25, C5-1, C5-0.5, C5-0.25, C3-1, C3-0.5, C3-0.25, CB7-1, CB7-0.5, CB7-0.25, CB5-1, CB5-0.5, CB5-0.25, CB3-1, CB3-0.5, CB3-0.25 and 3.75% Lugol's solution.

Preparations for this first test started with coding Falcon tubes (with a volume of 50 mL) and the tube lids with a marker and setting the tubes aside in a rack. After coding, pipet the right amounts of solutions in the coded Falcon tubes (see **Appendix V – Solutions without Tissue**).

Besides using different buffers also different buffer strengths were used (1x, 0.5x and 0.25x) as the outcome of using different buffer strengths has yet to be sorted out. The easiest way to prepare buffers of 1x, 0.5x and 0.25x is to start with a 2x buffer and combine and dilute appropriately. During this tests, pH, osmolarity and OD of the solutions were measured at predefined times (frequently over a period of about ten days). In the first test, no soft-tissue samples were used.

Preparations for a second test started with preparing the tissue samples via the conventional AMC method. The samples used were pieces of pork liver. Pork liver was chosen because of the following four reasons: i) it is easily available, ii) it has a homogeneous structure, iii) it can be easily (die) cut into equal samples and iv) Lugol's solution has binding affinity with haemoglobin which is abundantly present in liver tissue. Specifically the latter reason is important as the binding affinity of Lugol's solution leads to better CT imaging results. That liver tissue is imaged well with CT after staining is for instance also visible after staining a post-mortem human foetus with Lugol's solution. On the CT images the liver of the foetus is usually beautifully visible.

Continuing with the AMC method, the pork liver was cut into cubes, freshly dissolved in 4% w/v PFA in PBS (10 mM H_2NaPO_4/HNa_2PO_4, 150 mM NaCl, pH 7.40) to fixate at room temperature. After fixation, the liver cubes were stored in the refrigerator 0.2% PFA in PBS for a couple of days. Thereafter, the cubes were die cut into cylindrical shapes with a diameter of approximately 15 mm and a length of 20 mm. Via this die cutting method eighteen similar shapes were obtained. The cylindrical shaped liver samples were removed from the die cutting pot with tweezers. It is obviously important to not damage the samples too much with the sharp tips of the tweezers as it would impact the similarity of the samples. For the second test, five different buffered solutions[4] were made with a 1x buffer next to 3.75% w/v Lugol's solution. This buffer capacity was chosen due to the lowering of the pH of pure 3.75% w/v Lugol's solution and consequently to make sure that the solution has a better chance of staying within its buffer capacity. As noted before the lid plus tube were coded, after which the right amounts were pipetted into the tubes (see **Appendix VI – Pork Liver Tissue Test**).

After fixating and storage/cooling for a couple of days the pork liver samples have to be washed in PBS before they can be immersed in the staining solution. Washing is a common practice prior to the start of the staining procedure to remove excess free formaldehyde and enable the tissue to impregnate with buffer. [11] Washing starts with putting the samples in (for instance) empty Falcon tubes, adding PBS and shaking for ten seconds. Subsequently, the old PBS is replaced with new PBS in the tube after which it is let to rest on an electric shaker for 30 minutes. After the washing with PBS, all eighteen pork tissue samples are immersed in the six different staining solutions (three samples per staining solution). As soft-tissue that is not immersed will not be stained, it is important that the complete sample is immersed in a large amount of solution. As an AMC method guideline, use a solution volume of at least equal to twenty times the weight of the sample.

Besides regularly measuring pH for roughly ten days, osmolarity, OD and weight were measured. Additionally, CT scans of the pork liver samples were made to monitor staining progress, intensity of the staining and the volume of the samples. To perform CT scans, the samples were taken from their Falcon tubes (simply by using a small spoon) and positioned onto a paper towel to get rid of excess solution. The samples were positioned into a foam notch on top of a piece of paper (to avoid staining solution leaking into the foam). This "sample carrier" (see *Figure 8*) ensures that the samples are stably positioned while moving and during CT scanning.

[4] SB8-1, SB7-1, CB7-1, CB5-1 and CB3-1.

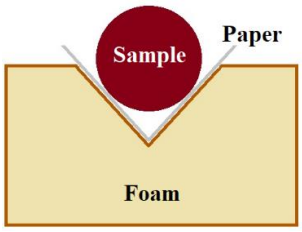

Figure 8 *Cross section of the sample carrier.*

In addition, a third test gave insight into what happened to the weight of the fixed pork liver samples when immersed in acidic solution only (in absence of Lugol's solution). Only weight measurements were performed as a proxy measurement because: i) weight loss generally shows the same trend as volume decrease (or tissue shrinkage) and ii) it is much easier and faster to perform compared to CT scanning and generating volume measurements. Acidic solutions used were only the CBs with a pH of 5.00 and 3.00 (n = 3). The results of this acidity test can then be compared to the results of the tests that does contain Lugol's solution.

The left side of *Figure 9* demonstrates a schematic overview of the AMC method staining protocol (fixation, storage, washing, staining).

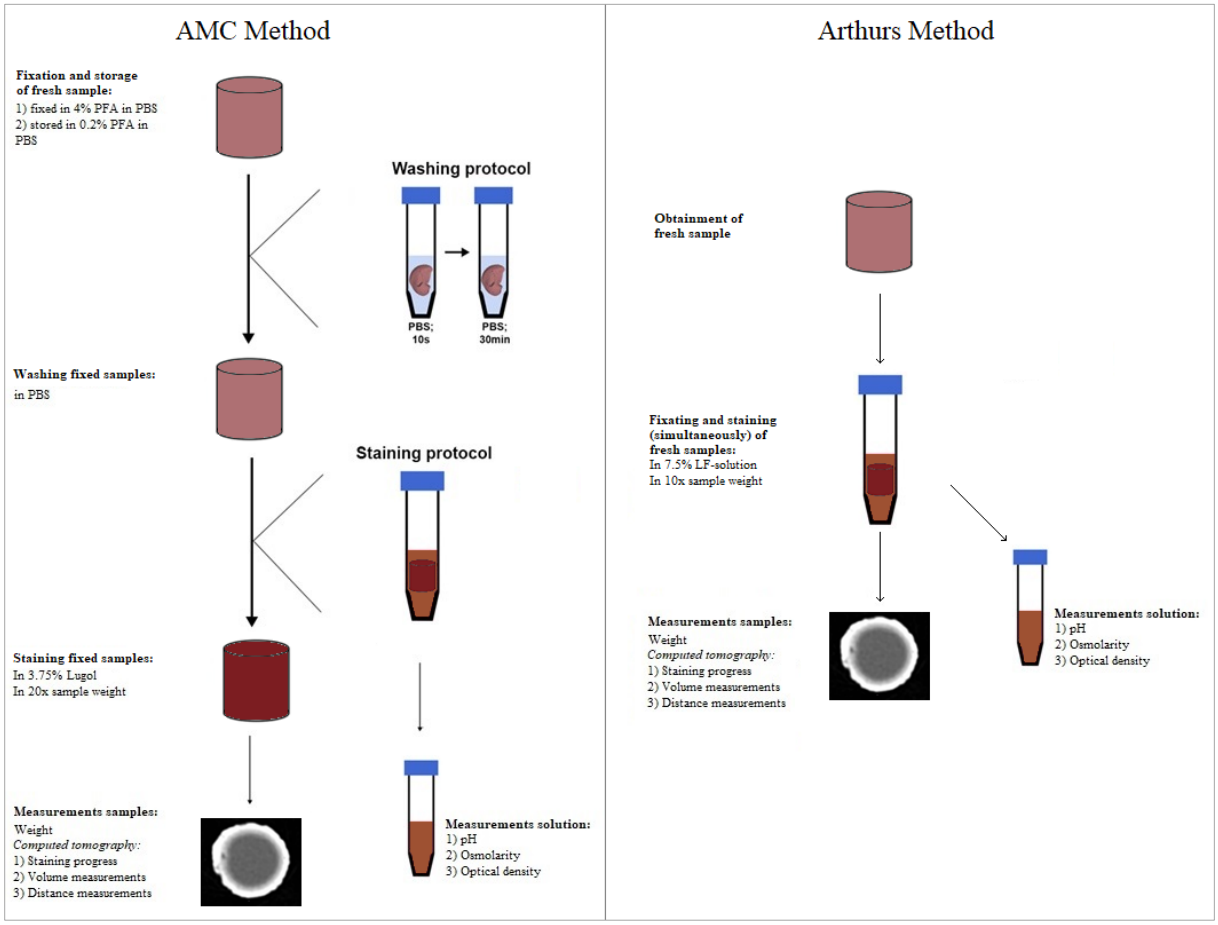

Figure 9 *Schematic overview of the AMC method and Arthurs method staining protocol.* ***Left****: conventional AMC method. Fresh samples are fixed first and then stored. After washing the samples are stained.* ***Right****: Arthurs method. Fresh samples are fixed and stained simultaneously, immediately after they are obtained. In both methods, the samples are weighted. Thereafter a CT scan is made to visually monitor staining process (by measuring distance/intensity) and measure sample volume (by measuring tissue shrinkage). pH, osmolarity and OD are measured during the staining process to closely monitor acidification, osmotic imbalance and Lugol's solution concentration.*

In short, the AMC method fixates the soft-tissue first and stains later (which is a conventional method), while Arthurs method uses a mixture of a fixative and stain simultaneously on fresh tissue. During the course of this study by means of the AMC method (as described above), Arthurs et al. published their

article *Human fetal whole-body post-mortem microfocus computed tomographic imaging* and claimed they had found no significant tissue distortion (no shrinkage) after they fixed and stained foetuses simultaneously in a LF-solution. [18] LF-solution consist out of 10% w/v formalin (for fixation and to halt tissue autolysis) and 15% w/v I_2KI (Lugol's solution for staining the tissue). To make the final staining solution, Arthurs et al. dilute the reagents mentioned above 1:1 which results into a total I_2 content of 63.25 mg/mL (= 7.5% w/v Lugol's solution concentration). The tissue is immersed into "a suitable volume" of I_2KI-formaline solution, which is approximately ten times the tissue weight (in comparison to the AMC method: twenty times the tissue weight is used). For example, foetuses below 100 g. are immersed in 1 L LF-solution and foetuses of 100 – 300 g. are immersed in 2.5 L LF-solution.

Since the goal of this study is to diminish soft-tissue shrinkage while using Lugol's solution as stain, Arthurs method is worth researching. Therefore a subsequent fourth test is performed in this study with fresh (no fixative used beforehand) pork liver samples. The fourth test is performed to find out if the solution that Arthurs et al. used indeed caused no significant tissue distortion (shrinkage). The right side of *Figure 9* demonstrates a schematic overview of the Arthurs method staining protocol. While performing Arthurs method, fifteen fresh pork liver samples were immersed in a different formalin (buffered) Lugol's solutions. Solutions used for this test were: LF-solution as described by Arthurs et al., a buffered version of the LF-solution (FBL), only formalin (F), a formalin buffered version (FB) and 7.50% Lugol's solution (L). A more detailed description of the solutions can be found in **Appendix VII – Arthurs Method**. Before starting the usual measurements, the pork liver samples were taken out of their Falcon tube and placed onto a disposable paper towel to eliminate excess surface fluid (approximately ten minutes). In the meantime, pH was measured. After pH measurements were completed, the pork liver samples were weighted and put back into their Falcon tubes. Osmolarity and OD measures were also performed.

Due to promising results with the pork liver samples, it was decided to also test Arthurs method on foetuses. During this study, two human foetuses (after TOPs), were donated to the Dutch Foetal Biobank (TOP175 (foetus #1): 15+4 weeks of gestation (weeks + days) and had a weight of 49.09 g. TOP176 (foetus #2): 19+6 weeks of gestation and had a weight of 286.17 g. After acquisition, at time point "T0" an MRI and CT were made as quickly as possible. Thereafter, the foetuses were immersed in LF-solution (1 L for TOP175, 2.5 L for TOP176). Once again, pH, osmolarity, OD and weight were measured. CT scans were made regularly at predefined time points until complete staining was achieved.

4.5 Soft-Tissue and Computed Tomography

To visualize homogeneous staining, staining intensity and soft-tissue shrinkage, CT imaging was used. The obtained DICOM-files were processed with recipes in the software package AMIRA (version 2020.2, Thermo Fisher Scientific, United States) to monitor staining progression visually and via a distance/intensity measurement to get the intensity line profiles (as explained in **2.3 Importance of Homogeneous Staining**) and measure volume to monitor tissue shrinkage. Below, the AMIRA recipes are elaborated on. Additional information about the AMIRA recipes workflow can be found in **Appendix VIII – AMIRA Recipes**.

Volume Measurements & Staining Progress of Pork Liver Samples

Performing the volume measurement AMIRA recipe, the measured volume is given per cylindrical shaped pork liver sample. The recipe starts with a resampling step, followed by two thresholding steps. The first thresholding step is necessary for two reasons: i) to find the transition from air to (stained) soft-tissue and ii) to fill holes which can be present in the pork liver samples (for example due to incomplete staining or unstained vessels). The second thresholding step, results into "completely filled" samples, which represents an overestimation of the total volume. To compensate for this overestimation, an erosion step is performed to shrink the volume beyond the first threshold limit. After eroding, the results of both thresholds are summed together, which leads to the most likely estimated volume. In the end, a

spreadsheet is created which contains information about the pork liver sample Z-position, it's volume, mean, median and index number. From this data, graphs are provided in which the volume (in mL) is plotted against staining time.

The distance/intensity measurement AMIRA recipe is used to visualise the staining progress and staining intensity via intensity line profiles. The intensity (in HU values) measured is plotted against the distance towards the centre of the pork liver samples. For instance, the distance of the pork liver samples is divided by rings, where the outer ring is number 1 and the most inner ring is a number greater than 1. The amount of rings depends on the diameter of the pork liver sample. See *Figure 10* for an example of ring numbering in a cross section of a pork liver sample with 25 rings. Each ring is approximately 0.25 mm.

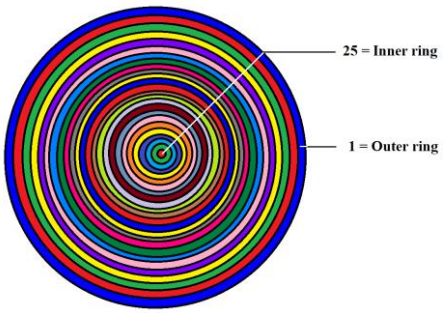

Figure 10 *Example of ring numbering in a cross section of a pork liver sample.*

During the execution of this recipe, thresholding is performed to make sure only the (stained) soft-tissue is measured. Small holes/spots are filled/removed from the sample, since they do not contribute to the staining progress measurements. The actual distance map is computed from a binary image (pixels that have only two possible intensity values) into a 3D distance field map. In the end, a spreadsheet is filled which contains information about the Z-position, staining intensity (in HU) and ring number. From this data, graphs can be made in which the staining intensity is plotted as an intensity line profile against the distance (ring number) for each time point.

Volume Measurements & Staining Progress of Foetuses
For the foetuses, a different approach is applied, since research was only performed on two foetuses. A "two step manual segmentation" is performed to calculate volume. Staining progress of the stained foetuses was objectively assessed via the CT images by visual inspection.

5. Results

In section **4.4 Tests on Different (Lugol's) Solutions**, three tests were described following the AMC method: i) solutions test without tissue, ii) pork liver samples test with an additional iii) acidity test and one test following Arthurs method (with pork liver and foetuses). In this section, the results of both methods are presented.

5.1 AMC Method: Solutions Without Tissue, Pork Liver Tissue & Acidity

The AMC method stains soft-tissue after fixation and washing.

Solution Test Without Tissue
First, Lugol's solution was mixed together with different buffers to study the acidification, osmotic balance and Lugol's concentration of the different mixed solutions. Measurements were conducted on pH, osmolarity and OD. The most important findings on acidity are that the pH values of 7.00, 5.00 and 3.00 remained stable over time, except for the 3.75% w/v Lugol's solution which did not contain a buffer (see *Figure 11*). The pH of Lugol's solution started at 6.64 and lowered to 5.03 (a decrease of 1.61) over a time period of 356.5 hours. Osmolarity and OD stayed approximately constant (these graphs can be found in **Appendix V – Solutions without Tissue**).

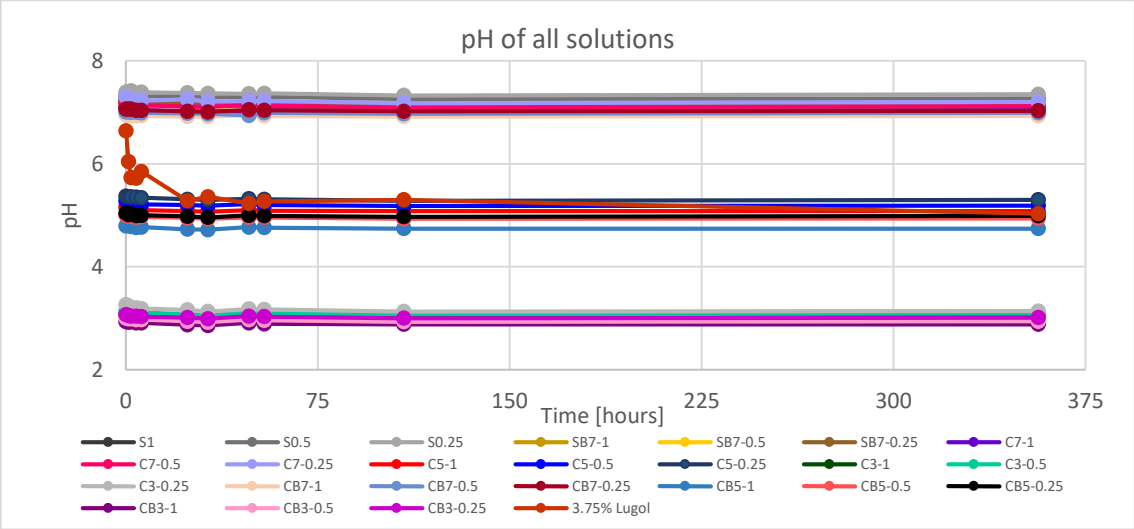

Figure 11 *pH measurement results (over time) of the solutions without tissue.*

Pork Liver Samples & Acidity Test

Pork liver samples were immersed in different (1x buffered) Lugol's solutions. Again, pH, osmolarity and OD were measured. In addition, the pork liver samples were weighted and CT scanned to monitor tissue shrinkage, staining intensity and staining progress. The pH values of SB7-1, CB7-1, CB5-1 and CB3-1 are considered relatively stable, their pH decreases maximally 0.90 over time. The pH values of SB8-1 and 3.75% w/v Lugol's solution are considered unstable, they decrease by 1.41 (from 8.04 to 6.63) and 4.94 (from 6.99 to 2.05) respectively. Regarding osmolarity, a slight increase over time can be observed. The OD values decreased over time. As regards to the pork liver samples' weight and volume, a weight loss of 30.00% and volume decrease of 35.00% can be observed over time (~250 hours) for samples immersed in acidic solutions (CB5-1, CB3-1 and 3.75% w/v Lugol's solution). Samples immersed in a neutral (pH 7.00) or more basic (pH 8.00) solution show a slight averaged increase over time of 5.58% in weight, and an averaged volume decrease of 4.82%. pH and volume measurements are demonstrated in *Figure 12* and *Figure 13*. The graphs show averages of three pork liver samples (n = 3), immersed in the same solution. Further results on osmolarity, OD graphs and weight measurement can be found in in **Appendix VI – Pork Liver Tissue Test**.

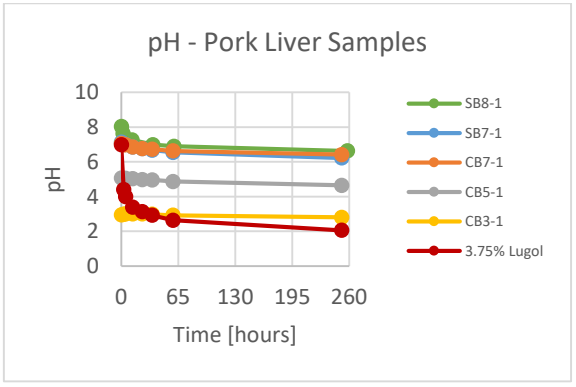

Figure 12 *Averaged pH over time (n = 3).*

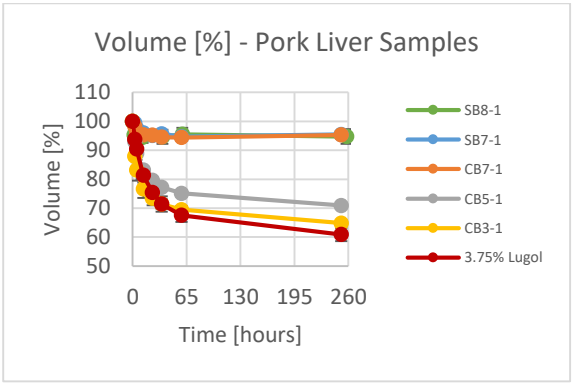

Figure 13 *Averaged volume over time (n = 3) (in percentages) relative to the starting volume.*

To visualise the staining progress, distance/intensity measurements were performed on each pork liver sample. One example of the distance/intensity measurement is presented in *Figure 14* by the intensity line profiles which is measured by the mean intensity (in *HU*) per ring. For each sample, the intensity line profiles can be found in **Appendix VI – Pork Liver Tissue Test**.

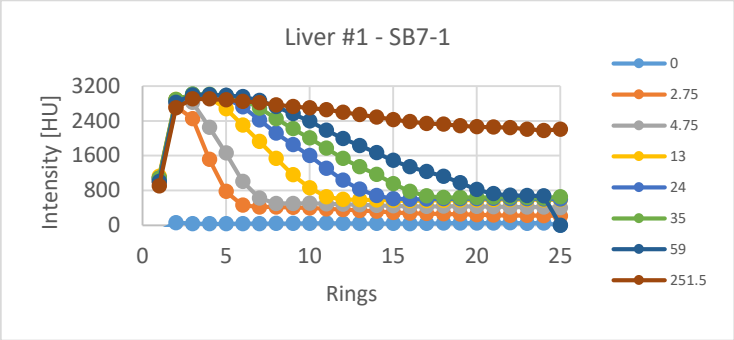

Figure 14 *Intensity line profile of pork liver sample #1 that was immersed in SB7-1 for 251.5 h. This graph is the result of the distance/intensity measurement performed via the AMIRA recipe.*

Tissue samples immersed in pH-neutral solutions or more basic solutions show a less homogeneous staining compared to tissue samples immersed in acidic solutions. Tissue samples in solution with lower pH values are stained quicker than tissue samples in solutions with a neutral/more basic pH value. These results are clearly visualised in *Figure 15*, where for the solutions with a pH of 7 or 8 (samples 01 to 03 and 1 to 6), the stain is taken up less quickly (less red in the figure).

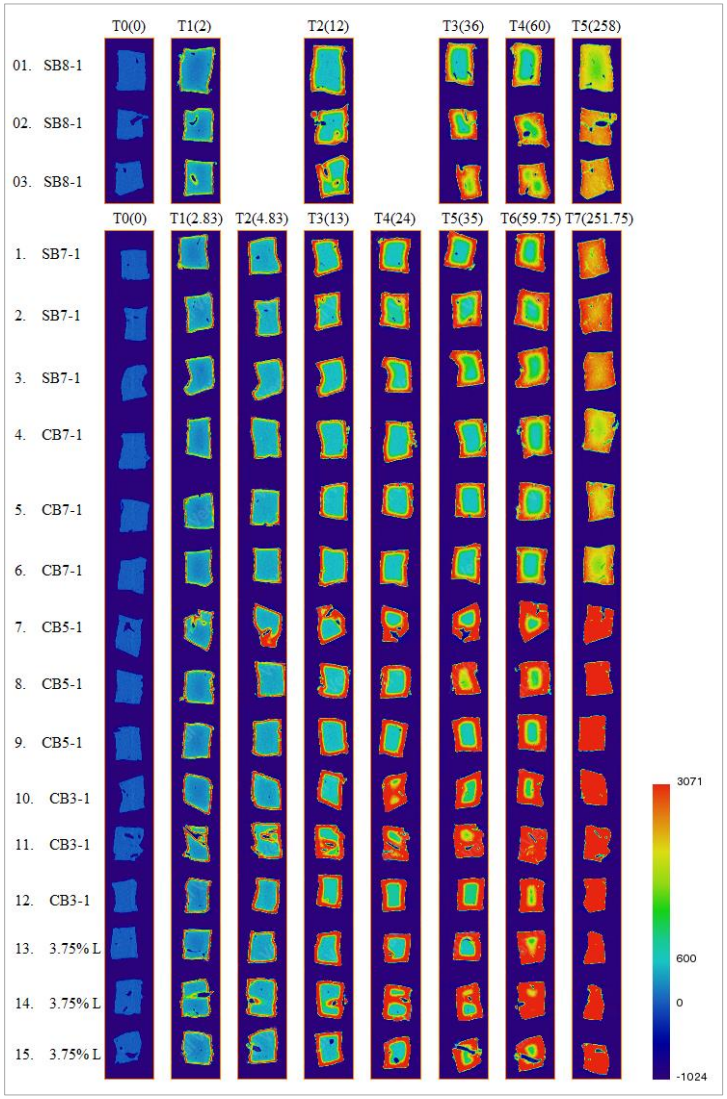

Figure 15 *Staining progress colour map of the pork liver samples over time (Time point(hours)). Intersections of the xz-plane. Blue: HU = -1024 (not stained). Red: HU = 3071 (maximum staining).*

Additionally, pork liver samples immersed in CB5 and CB3 acidic solutions (pH 5.00 and pH 3.00) were used to find out what happened to the sample weight in the absence of Lugol's solution. In *Figure*

16 a comparison can be seen between the tests that do (indicated with CBL) and do not contain Lugol's solution.

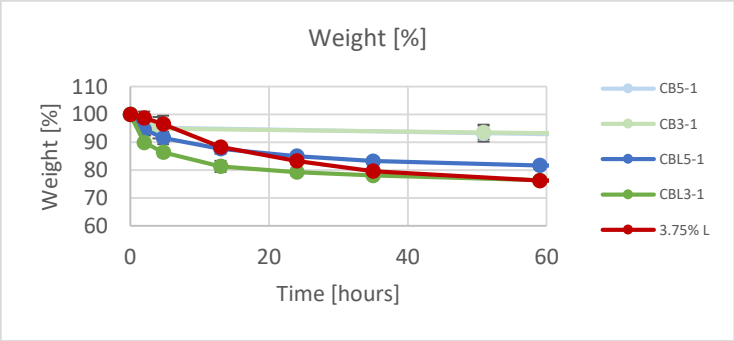

Figure 16 *Acidity test: comparison of acidic solutions without Lugol's solution (CB5-1 and CB3-1) and with Lugol's solution (CBL5-1, CBL3-1 and 3.75% L). Averages of three pork liver samples are shown, immersed in the same solution (n = 3).*

Comparing these results, both CB acidic solutions (without Lugol's solution) are more stable/maintaining their pH range. CB5-1 stays at pH = 5.00 (starting value 5.09, end value 5.07) and CB3-1 stays at pH = 3.00 (starting value 3.03, end value 3.13). The average weight loss of these samples is approximately 7%, compared to the 21% weight loss of acidic solutions that do contain Lugol's solution.

5.2 Arthurs Method: Pork Liver Samples & Foetuses

The Arthurs method stains and fixates fresh tissue simultaneously. At first, similar to the previous tests, pork liver samples were used as a first check, followed by two foetuses.

Pork Liver Tissue Tests

Fresh pork liver samples were immersed in different solutions and monitored up to ~190 *h.* staining time. As in previous tests the pH, osmolarity, OD and weight of the samples were measured. For efficiency purposes only one CT scan was made to check if the samples were stained thoroughly. For all measurements, averages of three pork liver samples are shown, immersed in five different solutions, resulting in fifteen pork liver samples in total.

In *Figure 17*, the pH results are presented. The pH of F- and FB-solution were relatively stable. The pH values started at 3.82 and ended at 4.36 (an increase of 0.54) for the F-solution and for the FB-solution pH values started at 7.05 and ended at 6.74 (a decrease of 0.31). Regarding the LF-, FBL- and L-solution, their pH is considered unstable. Starting values were 4.28, 6.88 and 6.45 and end values 2.22, 3.22 and 2.90 respectively.

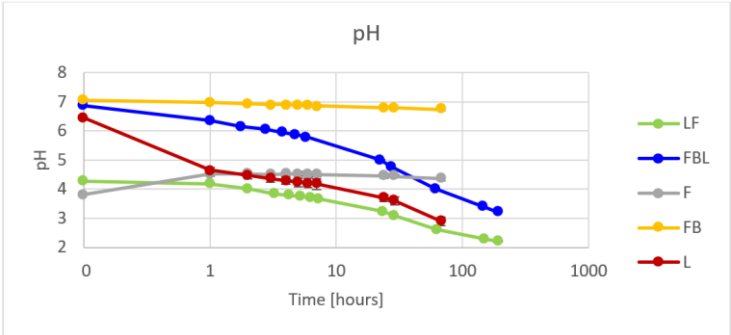

Figure 17 *Averaged pH over time (n = 3) of fresh pork liver samples.*

As expected, the osmolarity measurements, showed approximately the same results throughout the test. No significant increase or decrease was observed (see **Appendix VII – Arthurs Method**). Regarding the weight (see *Figure 18*) at first the weight increases, but over time the weight decreases. The overall decrease in weight is very small: approximately 3% for LF-solution.

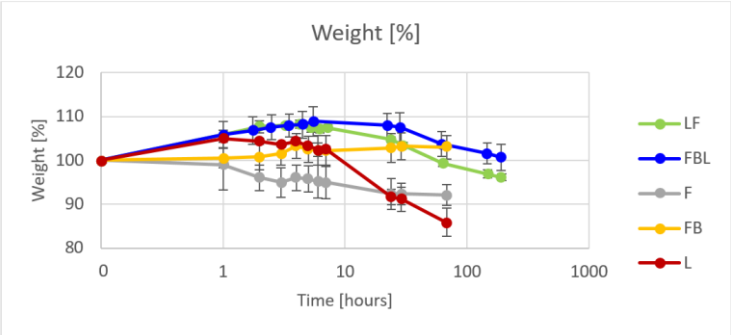

Figure 18 *Averaged weight over time (n = 3) of fresh pork liver samples (in percentages) relative to the starting weight.*

The OD measurements showed an unexpected increase over time, which can be seen in *Figure 19*. However, due to the promising results regarding a weight decrease of approximately 3% and regardless of the unexpected OD increase, it was decided to test the Arthurs method on foetuses. In *Figure 17 – Figure 19* , time is plotted at a logarithmic scale to better visualize the more frequently measured earlier time points.

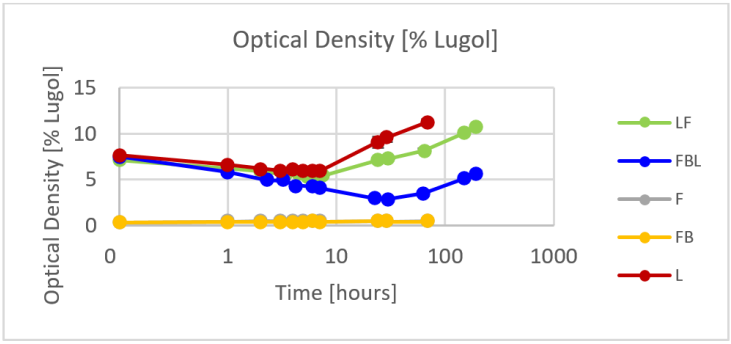

Figure 19 *Averaged optical density (n = 3) expressed in percentages Lugol's solution present in the solution.*

Foetuses

In the last test, two foetuses (TOP175 and TOP176) were stained with LF-solution according to Arthurs method. TOP175 (foetus #1): 15+4 weeks of gestation had a weight of 49.09 g. TOP176 (foetus #2): 19+6 weeks of gestation had a weight of 286.17 g. Over time, pH, osmolarity and OD of the LF-solution were measured. Additionally, the foetuses were weighted and CT scans were made to calculate volume and to monitor staining progress.

The pH decreased in both cases (see *Figure 20*). For TOP175 the pH decreased by 0.89 (from 4.07 to 3.18). The pH of TOP176 decreased by 0.92 (from 4.04 to 3.12). Osmolarity stayed approximately constant over time for TOP175. TOP176 showed a little increase in osmolarity over the first 25 hours, but thereafter stayed constant over time up until complete staining was achieved. OD showed, as expected, a decrease over time in both cases. Measuring the weight of the foetuses revealed that there was a large decrease in weight of 24.97% for TOP175 and only a small decrease in weight of 6.15% for TOP176. Further osmolarity, OD and weight results can be found in **Appendix VII – Arthurs Method**).

Measuring the volume of the foetuses (*Figure 21*), TOP175 revealed that there was a large decrease in volume of 31.94%. TOP176 showed little volume decrease of 1.08%. Analysis of the CT scans showed that all internal organs were completely and uniformly stained after 77 h. for TOP175 (see *Figure 22*) and 240.5 h. for TOP176 (see *Figure 23*). This difference in time is the obvious result as TOP175 is much smaller than TOP176 and is therefore more quickly stained.

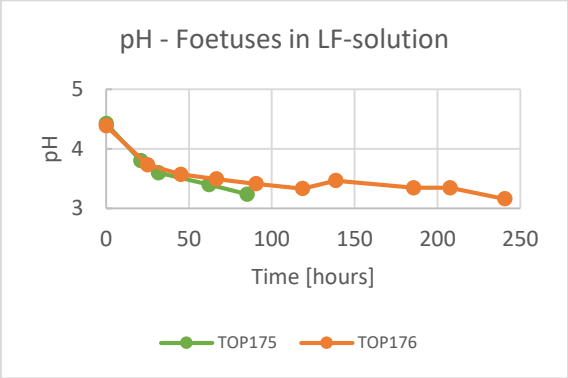

Figure 20 *pH over time of TOP175 and TOP176 in LF-solution.*

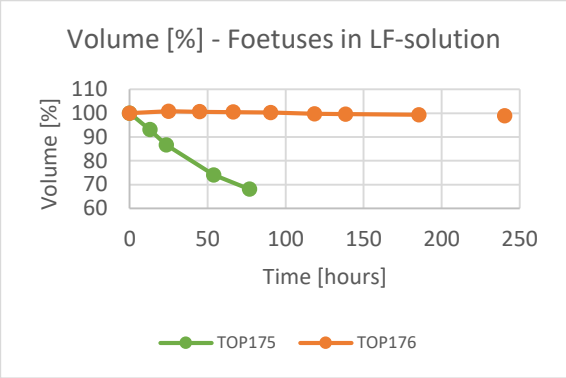

Figure 21 *Volume over time (in percentages) of TOP175 and TOP176 relative to the starting volume. The gap between 185.5 h. and 240.5 h. is because the CT scanner was out of use.*

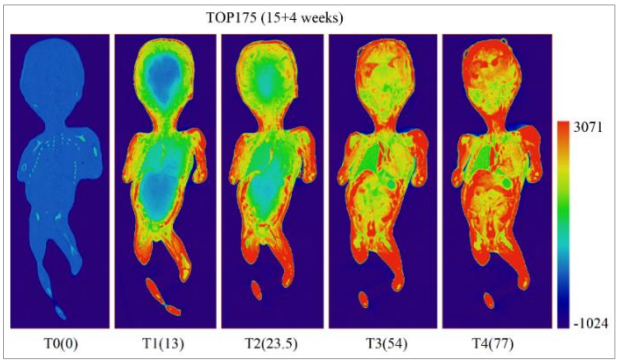

Figure 22 *TOP175: colour map of the staining progression until complete staining is achieved. Blue: HU = -1024 (not stained). Red: HU = 3071 (maximum staining).*

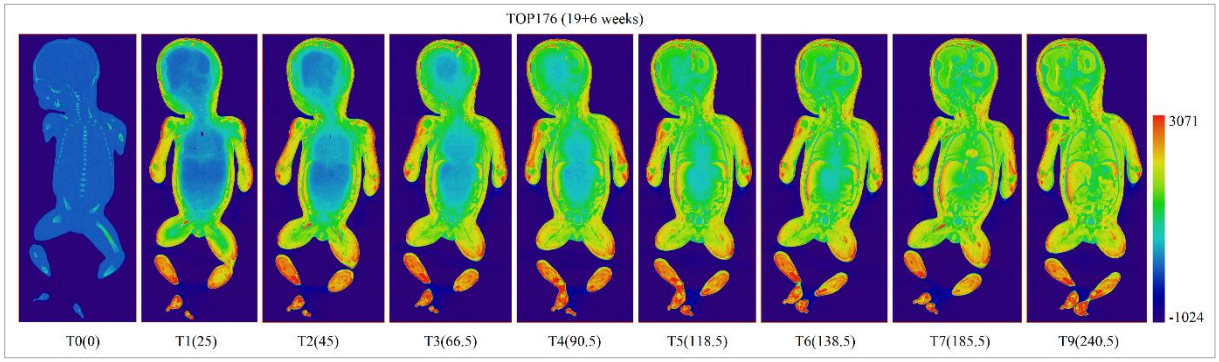

Figure 23 *TOP176: colour map of the staining progression until complete staining is achieved. Blue: HU = -1024 (not stained). Red: HU = 3071 (maximum staining).*

6. Discussion

This study focuses on diminishing soft-tissue shrinkage while optimising the Lugol's solution staining protocol for post-mortem human foetal imaging. Two methods (AMC and Arthurs) were applied. Their results are discussed below.

The AMC method demonstrated that pure Lugol's solution (3.75% w/v, without tissue) gets acidic over time. As acidification also happens to Lugol's solution stock on the shelf [11] it confirmed the expectations. Furthermore, the results showed no significant variance in pH value stability between the different buffer strengths. Even though the tests showed no variance, the strongest buffer (1x) was chosen to perform the follow-up tests as a precaution, as in principal a higher buffer capacity is better suited to keep the pH value stable. Osmolarity measurements show a slight increase over time. This increase can likely be assigned to the leakage of the fixative (PFA) from the pork liver samples, since

freshly dissolved 4% PFA in PBS has a high osmolarity of itself (1607 $mOsm$). [11] As expected, OD decreased during all measurements. The decrease of OD simply means that the concentration of Lugol's solution decreases over time, as triiodide binds to the pork liver samples. Visually this can be seen over time as the dark brown colour of Lugol's solution is slowly absorbed by the samples leaving a more transparent (residual) Lugol's solution behind. Pork liver samples immersed in neutral staining solutions show a slight weight increase of 5.58% on average, probably due to absorption of the solution. Volume however, shows an average decrease of 4.82%.

The acidic staining solutions show a higher staining intensity in the distance/intensity measurements (intensity line profiles). This is observed in the staining progress colour map of the pork liver samples (*Figure 15*). For the completely saturated samples, who were immersed in the more acidic solutions (given staining time) the question can be raised if the staining intensity is indeed stronger/more complete over the sample (from outer to inner ring) as the observed intensity for the full sample has simple reached the maximum of the range of the CT scanner used in this study (-1024;3071 HU). Simply said, if the maximum HU value of 3071 is reached for the full sample, every voxel will have the same maximum value and the sample will show up as a "red saturated blob" with low contrast. This is visible in *Figure 15* for samples that were immersed in CB5-1, CB3-1 and 3.75% w/v Lugol's solution after 251.75 h. (T7).

Lastly, the acidity tests demonstrated that solutions containing Lugol's solution result in more weight loss. Therefore, adding acidic Lugol's solution to any staining solution used in this study would suggest more weight loss and consequently more soft-tissue shrinkage.

Concerning Arthurs method non stable pH values were found for pork liver samples immersed in LF-, FBL- and L-solutions. These results also show that the buffer used in FBL-solution did not keep the pH stable. This is probably due to the buffer being too weak. To avoid this in future research, a stronger buffer (with a higher buffer capacity) could be used to further investigate. The weight of the pork liver samples increased at first, but later decreased in weight. Eventually, the weight was approximately stable with a 3% decrease. For the increase in weight it is assumed that the absorbed solution is weighted with the sample. The decrease was expected based on earlier tests as the lowering of the pH value would have that effect.

Unexpected were the Arthurs method results of the OD measurements. The expectation was a decrease of OD values after which the conclusion could be drawn that the concentration of Lugol's solution also decreased (due to the binding of triiodide to the tissue). This was also observed during the other tests via the AMC method. However, for Arthurs method, the opposite happened: an increase of OD values suggested an increase of Lugol's solution concentration (see *Figure 24*). Apparently the Nanodrop measured that over time the OD increases. Simply said the brown colour of the solution becomes darker brown over time. This darkening of the solution raises the question if the pork liver samples were stained thoroughly. To answer this question, a CT scan was performed (at t = 148.25 h.). From the colour map (see *Figure 25*) it can be seen that all samples (in LF- and FBL-solution) were stained thoroughly. Therefore it is assumed that the darkening of the solution has nothing the do with triiodide binding in the sample per se as the CT scans of the samples show intensity values of 75% (for FL-solution) and 79% (for FBL-solution) compared to the stock values.

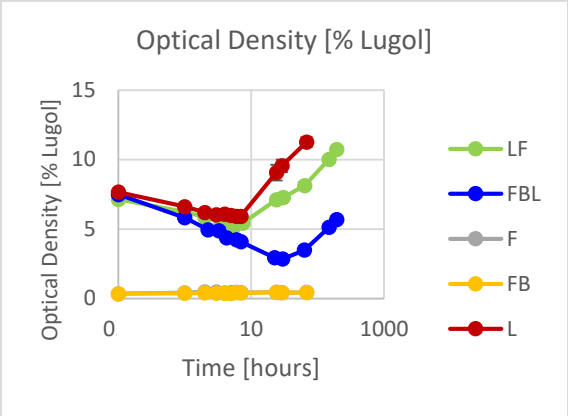

Figure 24 *Averaged optical density (n = 3) expressed in percentages Lugol's solution present in the solution.*

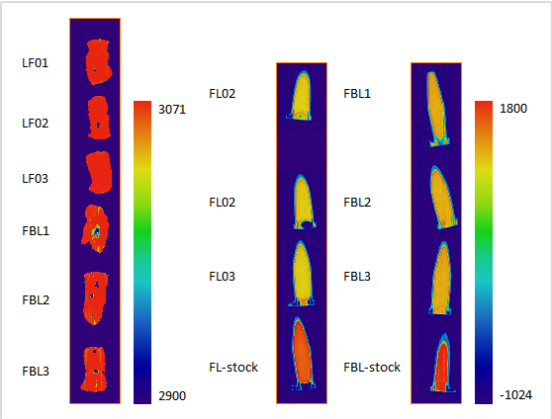

Figure 25 *Colour map of fresh pork liver samples to check if the staining is through. Blue means not yet stained, red means maximum staining.*

A plausible explanation could be that the sample leads to a reaction that eventually "leaks trough" to the solution it is immersed in. The University of Surrey provided an explanation that the darkening of the solution could be due to the presence of haemoglobin in the (pork liver) samples. The presence of haemoglobin leaking from the samples is highly likely due to simultaneously fixating and staining the samples (not using a fixative before immersing the sample in the staining solution) which is the case for Arthurs method. As haemoglobin reacts with the acidity in the tissue, it produces a precipitate of dark brown acid formaldehyde haematin. [33]

This explanation was tested by centrifugation of approximately 5 mL of all solutions as this technique would settle the precipitate. Centrifugation test results are presented in *Table 2*. Every solution shows an averaged (n = 3) difference in percentage Lugol's solution concentration, after centrifugation, varying between 1.37% and 3.33%, except the stock solutions where the difference is negligibly small. Since the Lugol's solution concentration starting value of this experiment was 7.5%, the differences are considered significant. Moreover, it can be concluded that for Arthurs method measuring the OD as proxy for Lugol's solution concentration may lead to unreliable estimations of staining uptake of the pork liver samples.

Table 2 *Centrifugation test: for each solution (n = 3) optical densities were measured before-, after- and without centrifugation. The differences between before- and after centrifugation are presented in the most right column.*

Solution	OD before centrifugation [% w/v Lugol]	OD Control measurement (without centrifugation)	OD after centrifugation	OD after centrifugation [% w/v Lugol]	OD difference before- and after centrifugation [%]
LF (n = 3)	12.01	1810.33	1598.00	10.64	1.37
FBL (n = 3)	6.81	1005.67	759.33	5.21	1.59
L (n = 3)	13.25	2002.33	1486.67	9.92	3.33
7.5% L stock	7.27	1078	1068	7.21	0.06
FL stock	6.57	969	963	6.53	0.04

The foetuses stained according to Arthurs method, show differences in staining time until complete staining was achieved. The observed difference in staining time is correlated with specimen size, the larger the specimen, the longer the required staining time to achieve complete staining. Comparing TOP175 to TOP176, the large difference in shrinkage (relative to its weight and volume) is assumed to be due to the abnormalities of TOP175. The skin of TOP175 was not intact and the lungs grew outside the foetus' body (on its back). In addition, since TOP175 of 15+4 weeks of gestation does not have a fully developed skin yet, it is suggested that the maturity of the skin is an important factor. This applies to both the time it takes to reach complete staining (mature skin takes longer) and prevent shrinkage by

having a “natural” barrier. According to literature, a non-penetrant stratification of the skin is complete when the foetus is 19 weeks old. [34], [35] These assumptions are substantiated by the CT scan results of TOP176 of 19+6 weeks of gestation with a mature skin. TOP176 shows little shrinkage of 1.08% and achieved homogeneous staining after longer staining time compared to TOP175. It is however unclear to what extent the skin maturation influences staining time, as TOP176 was also much bigger (in volume) than TOP175.

Considering all the tests, the results do not provide a clear explanation if the hypothesis of keeping the pH value of Lugol’s solution neutral will prevent tissue shrinkage. Since the relatively acidic LF-solution in Arthurs method started at a pH value of 4.04 and only little shrinkage of tissue occurred, further research is necessary to figure out as to why. A possible explanation could be that it has to do with how much the pH value drops, rather than at what pH value the staining starts (flow versus stock).

7. Conclusion

The goal of this study was to develop an optimum (buffered) Lugol’s solution staining protocol for post-mortem human foetal CT imaging to achieve homogeneous staining and diminish soft-tissue shrinkage, considering staining solution concentration, staining time and specimen size (*Main question*). The AMC method that uses neutral buffered staining solutions sounded promising. However, the recently published Arthurs method showed even more promising results. Both methods lead to homogeneous staining, but the AMC method leads to larger shrinkage of the tissue, considering staining solution concentration, staining time and specimen size. For the AMC method it is best to use a pH-neutral buffered Lugol’s solution, for example a SB7-1 Lugol’s solution, since shrinkage was limited to 4.82%. Arthurs method is considered a better option because fixating and staining simultaneously – using the LF-solution – resulted in a shrinkage of only 1.08% (for a foetus with mature skin). In addition, Arthurs method is more time efficient than the AMC method. Notwithstanding the above, it is important to keep in mind that staining success depends on three factors that influence each other: specimen size, used staining solution concentration and staining time. Even though all these factors were considered, the research was not extensive enough to address them all separately. This is why further research is warranted.

This study started with answering the sub-question on difference in pH stability over time for normal-, SB- and CB-Lugol’s solution. From these experiments, performing the AMC method, it is concluded that the different buffered solutions with different buffer strengths (0.25x, 0.5x and 1x) had no significant variance in pH over time. Even though this conclusion was reached, out of precaution the 1x buffer (the strongest) was used for further testing and answering the first sub-question. The second sub-question focused on diminishing the shrinkage artefacts on fixed pork liver samples by comparing buffered Lugol’s solution to normal Lugol’s solution. In follow-up tests this indeed seemed to be the case: stable pH values lead to the least amount of soft-tissue shrinkage. Pork liver samples immersed in normal Lugol’s solution showed the highest percentage of tissue shrinkage of 39.16%. As to the difference between SB or CB Lugol’s solutions, it was found that the amount of pork liver sample shrinkage was dependent on the initial pH value and not on which buffer was used. Pork liver samples immersed in acidic solutions showed 35.00% shrinkage on average. Samples immersed in a neutral or more basic solution shrunk 4.82%. The tests did show that the samples immersed in neutral or more basic solutions had a somewhat less homogeneous staining compared to tissue samples immersed in acidic solutions. So specifically for a homogeneous staining result, it would seem that more acidic solutions are preferred. However, as noted this comes at the cost of more tissue shrinkage.

Optimising the staining protocol is a continuous process for which further research will lead to better insights. This is also evidenced by the new Arthurs method and tests performed by this study. Part of the reason that optimising the staining protocol is a continuous process is due to the multiple factors that affect each other and the outcome of the staining protocol. Suggestions for future research are therefore

abound, but based on this study the most obvious are: i) research on what effect different concentrations of (buffered) Lugol's solutions will have on soft-tissue shrinkage, ii) testing Arthurs method on fixed tissue instead of fresh tissue as conducted in the AMC method (combining "the best of both worlds") and iii) specifically based on this study with the staining of foetuses, perform the Arthurs method on more foetuses in different gestation ages to find out about the role of skin maturation in the staining process.

References

[1] B. S. De Bakker *et al.*, "An interactive three-dimensional digital atlas and quantitative database of human development," *Science (80-.).*, vol. 354, no. 6315, 2016, doi: 10.1126/science.aag0053.

[2] K. Degenhardt, A. C. Wright, D. Horng, A. Padmanabhan, and J. A. Epstein, "Rapid 3D phenotyping of cardiovascular development in mouse embryos by micro-CT with iodine staining," *Circ. Cardiovasc. Imaging*, vol. 3, no. 3, pp. 314–322, 2010, doi: 10.1161/CIRCIMAGING.109.918482.

[3] B. D. Metscher and G. B. Müller, "MicroCT for molecular imaging: Quantitative visualization of complete three-dimensional distributions of gene products in embryonic limbs," *Dev. Dyn.*, vol. 240, no. 10, pp. 2301–2308, 2011, doi: 10.1002/dvdy.22733.

[4] P. M. Gignac *et al.*, "Diffusible iodine-based contrast-enhanced computed tomography (diceCT): An emerging tool for rapid, high-resolution, 3-D imaging of metazoan soft tissues," *J. Anat.*, vol. 228, no. 6, pp. 889–909, 2016, doi: 10.1111/joa.12449.

[5] B. D. Metscher, "Micro CT for comparative morphology: Simple staining methods allow high-contrast 3D imaging of diverse non-mineralized animal tissues," *BMC Physiol.*, vol. 9, no. 1, 2009, doi: 10.1186/1472-6793-9-11.

[6] B. D. Metscher, "MicroCT for developmental biology: A versatile tool for high-contrast 3D imaging at histological resolutions," *Dev. Dyn.*, vol. 238, no. 3, pp. 632–640, 2009, doi: 10.1002/dvdy.21857.

[7] Y. Dawood, G. J. Strijkers, J. Limpens, R. J. Oostra, and B. S. de Bakker, "Novel imaging techniques to study postmortem human fetal anatomy: a systematic review on microfocus-CT and ultra-high-field MRI," *Eur. Radiol.*, vol. 30, no. 4, pp. 2280–2292, 2020, doi: 10.1007/s00330-019-06543-8.

[8] P. Vickerton, J. Jarvis, and N. Jeffery, "Concentration-dependent specimen shrinkage in iodine-enhanced microCT," *J. Anat.*, vol. 223, no. 2, pp. 185–193, 2013, doi: 10.1111/joa.12068.

[9] S. De Bournonville, S. Vangrunderbeeck, and G. Kerckhofs, "Contrast-enhanced microCT for virtual 3D anatomical pathology of biological tissues: A literature review," *Contrast Media Mol. Imaging*, vol. 2019, pp. 5–6, 2019, doi: 10.1155/2019/8617406.

[10] J. C. Hutchinson *et al.*, "Postmortem microfocus computed tomography for early gestation fetuses: a validation study against conventional autopsy," *Am. J. Obstet. Gynecol.*, vol. 218, no. 4, pp. 445.e1-445.e12, 2018, doi: 10.1016/j.ajog.2018.01.040.

[11] Y. Dawood *et al.*, "Reducing soft tissue shrinkage artefacts caused by staining with Lugol's solution," pp. 1–18.

[12] P. Heimel *et al.*, "Iodine-enhanced micro-CT imaging of soft tissue on the example of peripheral nerve regeneration," *bioRxiv*, vol. 2019, 2018, doi: 10.1101/477539.

[13] Y. Dawood and B. S. de Bakker, "Micro-CT of early human development," *Radiology*, vol. 297, no. 1, p. 32, 2020, doi: 10.1148/radiol.2020201660.

[14] Lumen: Boundless Biology, "Osmoregulation and Osmotic Balance." [Online]. Available: https://courses.lumenlearning.com/boundless-biology/chapter/osmoregulation-and-osmotic-balance/. [Accessed: 24-Jun-2021].

[15] Lumen, "Buffer Solutions." [Online]. Available: https://courses.lumenlearning.com/boundless-chemistry/chapter/buffer-solutions/.

[16] C. LibreTexts, "Introduction to Buffers," 2020. .

[17] Chemistry, "Buffers." [Online]. Available: https://opentextbc.ca/chemistry/chapter/14-6-buffers/. [Accessed: 26-May-2021].

[18] I. C. Simcock, S. C. Shelmerdine, J. C. Hutchinson, N. J. Sebire, and O. J. Arthurs, "Human fetal whole-body postmortem microfocus computed tomographic imaging," *Nat. Protoc.*, vol. 16, no. 5, pp. 2594–2614, 2021, doi: 10.1038/s41596-021-00512-6.

[19] L. Hrvoje and M. W. Greenstaff, *X-Ray Computed Tomography Contrast Agents*, vol. 113, no. 3. 2014.

[20] J. L. P. and J. M. Links, *Medical Imaging Signals and Systems*. 2015.

[21] E. Descamps, A. Sochacka, B. de Kegel, D. Van Loo, L. Hoorebeke, and D. Adriaens, "Soft tissue discrimination with contrast agents using micro-ct scanning," *Belgian J. Zool.*, vol. 144, no. 1, pp. 20–40, 2014, doi: 10.26496/bjz.2014.63.

[22] J. Brodeur and R. Tardif, *Encyclopedia of Toxicology (Second Edition)*. Elsevier, 2005.

[23] Khan Academy, "Diffusion and Passive Transport." [Online]. Available: https://www.khanacademy.org/science/ap-biology/cell-structure-and-function/facilitated-diffusion/a/diffusion-and-passive-transport. [Accessed: 15-Jun-2021].

[24] T. D. Butters *et al.*, "Optimal iodine staining of cardiac tissue for X-ray computed tomography," *PLoS One*, vol. 9, no. 8, pp. 1–6, 2014, doi: 10.1371/journal.pone.0105552.

[25] J. Martins De Souza E Silva *et al.*, "Dual-energy micro-CT for quantifying the time-course and staining characteristics of ex-vivo animal organs treated with iodine-and gadolinium-based contrast agents," *Sci. Rep.*, vol. 7, no. 1, pp. 1–10, 2017, doi: 10.1038/s41598-017-17064-z.

[26] R. Balint, T. Lowe, and T. Shearer, "Optimal contrast agent staining of ligaments and tendons for X-ray computed tomography," *PLoS One*, vol. 11, no. 4, 2016, doi: 10.1371/journal.pone.0153552.

[27] P. G. Cox and C. G. Faulkes, "Digital dissection of the masticatory muscles of the naked mole-rat, heterocephalus

glaber (Mammalia, Rodentia)," *PeerJ*, vol. 2014, no. 1, pp. 1–19, 2014, doi: 10.7717/peerj.448.
[28] Amsterdam UMC, "Medisch Ethische Toetsings Commissie (METC)." [Online]. Available: https://www.amc.nl/web/research-75/medisch-ethische-toetsings-commissie-metc.htm.
[29] Amsterdam UMC, "Donatie van foetussen." [Online]. Available: https://www.amc.nl/web/nieuws-en-verhalen/verhalen/community/donatie-van-foetussen.htm.
[30] ConsortNV, "CONSORT Manual P901," 2002.
[31] ThermoScientific, "NanoDrop 1000 Spectrophotometer V3.8 User's Manual," 2010.
[32] Salmenkipp, "Osmometers Cryoscopic." [Online]. Available: https://www.salmen-kipp.nl/index.php/component/virtuemart/osmometers/cryoscopic. [Accessed: 26-May-2021].
[33] University of Surrey, "Formalin Fixative." [Online]. Available: https://www.surrey.ac.uk/sites/default/files/Formalin-Fixative.pdf. [Accessed: 31-May-2021].
[34] M. S. Hu *et al.*, "Embryonic skin development and repair," *Organogenesis*, vol. 14, no. 1, pp. 46–63, 2018, doi: 10.1080/15476278.2017.1421882.
[35] N. A. Coolen, K. C. W. M. Schouten, E. Middelkoop, and M. M. W. Ulrich, "Comparison between human fetal and adult skin," *Arch. Dermatol. Res.*, vol. 302, no. 1, pp. 47–55, 2010, doi: 10.1007/s00403-009-0989-8.
[36] Khan Academy, "Osmosis and Tonicity." [Online]. Available: https://www.khanacademy.org/science/ap-biology/cell-structure-and-function/mechanisms-of-transport-tonicity-and-osmoregulation/a/osmosis. [Accessed: 15-Jun-2021].

List of Figures

List of Tables

Appendices

Appendix I – Literature Study

Staining for µCT Scanning (in Foetal Imaging)

Tessa de Vries (4749928)

Keywords Computed Tomography, contrast, foetal imaging, iodine, Lugol's solution, osmium tetroxide, polyoxometalate, phosphomolybdic acid, phosphotungstic acid, staining.

Abstract Biomedical researchers and clinicians are interested in (ab)normal foetal development to better understand human anatomy. Traditionally, the combination of histological sectioning and confocal microscopy is used to create three dimensional (3D) images. However, besides being destructive downsides are possible tissue distortion and time consuming image reconstruction. Since 2009, non-destructive 3D imaging techniques like micro computed tomography (μCT) have been introduced to achieve higher resolutions in relatively short scanning times. Visualising soft-tissues remains a challenge due to low X-ray absorption. Therefore, chemical compounds (stains/contrast agents) that contain elements with high atomic numbers are used to enable soft-tissue visualisation. Because many stains are available, this literature study provides an overview of widely used stains and shortly addresses the relevant staining protocols to study post-mortem (human) foetal anatomy. The aim of this literature study is to i) provide information about the most frequently used stains and consequently ii) analyse relevant success factors at each step of the staining protocol. Most frequently used stains are: Lugol's solution (I_2KI), osmium tetroxide (OsO_4), phosphotungstic acid (PTA), phosphomolybdic acid (PMA) and Hafnium-based Wells–Dawson polyoxometalate (Hf-POM). Weighing the advantages against the disadvantages, Lugol's solution is considered the best option for μCT staining in post-mortem (human) foetal imaging. Protocol wise, staining success depends on three factors influencing each other: specimen size, staining solution concentration and staining time. Individually researching these success factors, calculating staining speed and objectively assessing staining homogeneity are suggested for further research. The combination of the successes found will thereafter lead to the "most optimal" staining protocol for post-mortem (human) foetal μCT imaging.

Nomenclature

3D	Three Dimensional
µ	Micro
AMC	Academisch Medisch Centrum
CT	Computed Tomography
EM	Electron Microscope
Hf-POM	Hafnium-based Wells–Dawson polyoxometalate
PBS	Phosphate Buffered Saline solution
PMA	Phosphomolybdic acid
POMs	Polyoxometalates
PTA	Phosphotungstic acid

AMSTERDAM U 2nd of February, 2021

Meibergdreef 9, 1105 AZ, Amsterdam
Supervision: Yousif Dawood

Introduction

Foetal development is essential for understanding human anatomy. During embryonic development, the arrangement of organs in the body is laid down. Having three dimensional (3D) insight into this formation, biomedical researchers and clinicians can be informed about (ab)normal development. [1] Traditionally, these studies were performed on histological analysis of sectioned specimens. [2] To create 3D images, two methods are combined: histological sectioning followed by confocal microscopy. This combination copes with possible tissue distortion and is very time consuming due to the necessary section alignment. [3] Since 2009, non-destructive 3D imaging methods are introduced to enable high resolution imaging in shorter time periods compared to histological sectioning/microscopy. One of the methods used to achieve these results is micro computed tomography (μCT), with a voxel resolution of 1 - 100 μm. [3] However, inherent to computed tomography (CT), soft-tissue provides less contrast in the images. Therefore, it is necessary to stain soft-tissues with a contrast solution to enable visualisation. [4]

This study provides an overview of current stains/staining protocols to enhance μCT contrast that study post-mortem (human) foetal anatomy. The aim of this literature study is to i) provide information about the most frequently used stains and consequently ii) analyse the relevant success factors at each step of the staining protocol. This study is performed with the use of Google Scholar and PubMed.

In this study, background information is given about (the working of) (μ)CT and the use of contrast agents (Section 1), followed by the applied method (Section 2) and results (Section 3). Finally, the conclusion with suggestions for future research is given in Section 4.

Background Information

Computed tomography (CT) is a non-invasive diagnostic tool that allows for 3D (visual) reconstruction/segmentation of tissues of interest. [5]–[8] In conventional CT, a rotating X-ray source is used to reconstruct cross-sectional images of the anatomy. The X-ray photons originate from an X-ray tube and travel on to the scanned specimen where they interact with matter. [9][10] The radiation that goes through the specimen without any interaction is measured and can be described by the Beer-Lambert law (*Equation 1*):

$$I_\theta(r) = I_0 \cdot e^{-\int \mu \cdot x \, dx} \quad \textbf{(1)}$$

Where $I_\theta\ (r)$ is the intensity of the outgoing beam, I_0 the intensity of the incoming beam, μ being the (varying) attenuation coefficient in $[m^{-1}]$ (the probability of having an interaction) and x the thickness of the slice in $[m]$. Thereafter, an anti-scatter grid ensures that only photons that did not scatter go through [11] and are measured by a detector (in intensity). To create the actual image, multiple image reconstruction methods [12][13] are available but these methods are not elaborated upon further in this study.

μCT scanners have a smaller field-of-view compared to conventional CT scanners, they work similarly, but there is one major difference. In μCT scanning, the specimen is being rotated and parameters such as "object-to-detector" and "source-to-object" distances are adjustable. These adjustments allow for greater magnification and higher resolution with μCT (1 - 100 μm) compared to conventional CT (0.5-1 mm). Another advantage of using μCT is quickly providing high-resolution images without performing histological sectioning and confocal microscopy. [7][8] Because of the non-destructive nature of CT, it can also be combined with other imaging techniques or the specimen can be rescanned if necessary. For instance, if histological sectioning is desired this could still be performed after scanning. Furthermore, μCT scanning provides images that preserve a complete set of image data, the technique is widely available and relatively inexpensive.

However, as X-rays are attenuated more by denser tissues (for example bone), and easily pass through low density structures, it is harder to visualize soft-tissues. The problem in differentiating between soft-tissues is that the difference in the attenuation coefficients is small. Contrast enhancement of soft-tissue can be achieved by the use of contrast agents also known as stains. [14][15] Stains can be used to distinguish between different (soft) tissues. Stains of interest are the ones that can evaluate tissue/organ function or performance, provide specific biochemical information or increase sensitivity and enhance differentiation. To achieve higher levels of X-ray attenuation for soft-tissue, high density fluids with a high atomic number are mostly used. *Equation 2* explains why these specific fluids have higher attenuation:

$$\mu \approx \frac{\rho Z^4}{A E^3} \qquad \textbf{(2)}$$

In this formula, ρ represents the density [kg/m^3], Z the atomic number, A the atomic mass and E the X-ray energy. The biggest contributor is the Z^4 factor, which allows for contrast levels of several orders of magnitude between different tissues and types of contrast. [15]

Lastly it is noted that staining uptake happens over time by relying on passive diffusion. Therefore, staining success depends on the specimen size, used staining solution concentration and staining time. [4]

Method

Finding useful literature to support the main goal of this literature study was done in multiple phases. To begin with, general information was gained on the operation of (μ)CT scanning. This was mostly done with the use of books and (online) lectures. [5]–[7], [9], [10], [13], [16] Thereafter, two articles from Metscher et al. [14], [17] served as a basis. Those articles explain different staining protocols that allow higher contrast with the use of μCT. One of the main points of interest is the use of different stains/contrast agent.

Since this literature study focusses on most frequently used stains and success factors at each step of the staining protocol, Google Scholar and the PubMed database were used to find relevant literature.

As search criteria, the following keywords were used: “(micro)CT”, “staining”, “contrast agent”, “imaging”, “iodine”, “Lugol’s solution”, “osmium tetroxide”, “phosphotungstic acid”, “Foetal”, “Anatomy” and “Postmortem”. Most of the time, combinations of these criteria were used. For example: “osmium tetroxide stain CT” and “Lugol solution CT imaging”. Because of many hits and a limited time scheme, a selection was made of the most relevant material for this study.

Results

This section contains the results gathered in the literature study. **Section 3.1 Stains** provides information on most frequently used stains (Lugol’s solution, osmium tetroxide, phosphor-acids and polyoxometalates), followed by **Section 3.2 Staining Protocol** that explains the generalised steps of a staining protocol (fixation, staining and imaging) and their success factors.

3.1 Stains

Lugol’s Solution

The most commonly used staining solution is called Lugol’s solution, a mixture of one part iodine and two parts potassium iodide in water (I_2KI). Heimel et al. report that Lugol’s solution stains glycogen, which has a remarkably high binding capacity to iodine. Moreover, Lugol’s solution can be used to identify full-size nerve samples, as iodine also binds to carbohydrates and lipids (which can be found a.o. in myelinated nervous tissue). An advantage of using Lugol’s solution is that the staining protocol is very simple compared to other protocols. A downside of using Lugol’s solution is the concentration-dependent tissue shrinkage after immersing the tissue into the I_2KI solution. A higher Lugol’s solution

results into a more rapid and larger volume decrease. [18] It is found by Dawood et al. that most researchers use an isotonic concentration of (at the most) 3.75% Lugol's solution, there will be neither shrinking or swelling of the cells. [4]

In general it can be assumed that in small specimens the Lugol's solution stain has a small distance to travel to reach the internal soft-tissues. This results into low staining concentrations and relatively short staining times. Another option is to stain with a higher concentration for a shorter period of time, but this will increase the chance of tissue shrinkage and overstaining (which can occur at 10% w/v concentration of Lugol's solution). [18],[21] Another frequently occurring staining step is rinsing/washing the specimen samples with (double distilled) water to remove excess surface stain from the specimen. [3],[17],[21]

Furthermore, using Lugol's solution as stain is cost-effective, reversible and more importantly a nontoxic option for contrast enhancement of soft-tissues. [2],[21],[22],[23] An example of a μCT image of a human foetus with and without Lugol's solution staining is illustrated in *Figure 1*. [2][4]

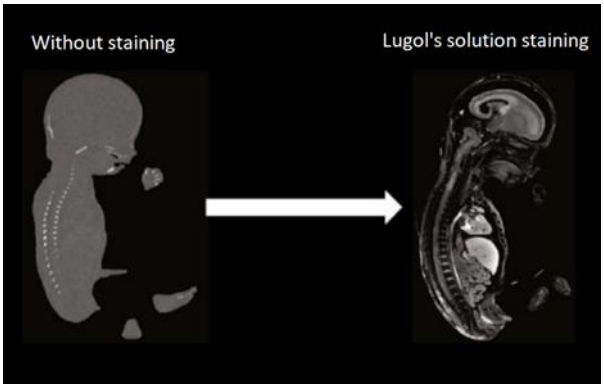

Figure 1 *μCT images of a human foetus illustrating the increase of soft-tissue visualization due to Lugol's solution staining. Left: without staining. Right: with Lugol's solution staining. [4]*

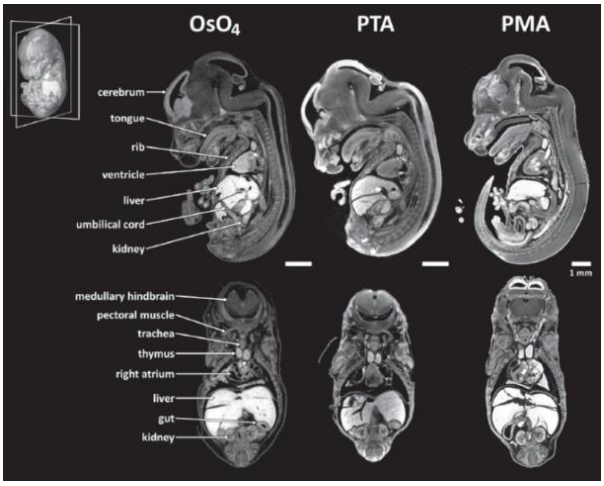

Figure 2 *μCT images of a mouse embryo, stained with osmium tetroxide (OsO_4), phosphotungstic acid (PTA) and phosphomolybdenic acid (PMA). Sagittal section is shown on the top, frontal section is shown on the bottom. [24]*

Osmium tetroxide

Osmium tetroxide has the chemical formula OsO_4. In its pure form, it is colourless, highly poisonous and suitable for a wide range of organic solvents. In 1952 G.E. Palade was the first to use osmium tetroxide in identifying the structure and function of cell organelles using the electron microscope (EM). [25] Osmium tetroxide can be used as a fixative and as a dye. Using it as a dye, it will bind to lipids because it is soluble in fats. By the addition of double carbon-to-carbon bonds, osmium tetroxide is reduced and metallic osmium is deposited in the tissue (as a black reduction compound). [26] Besides visualizing fats, also myelinated nerve fibres react strongly. Descamps et al. made an overview of the

published binding preferences of stains and the level of visualization that is obtained. This overview is used as a basis and supplemented with information from other stains (see *Table 1*). They also added a μCT image of an osmium tetroxide stained mouse embryo (left side of *Figure 2*). [24] In μCT imaging, osmium tetroxide will be visualized as opaque because it is a heavy metal. [25]–[27] Furthermore, osmium tetroxide is a potential candidate for X-ray contrast staining because of the K-shell energy of 73.9 keV, which is an electron binding energy favourable for strong X-ray absorption. [14] Also, osmium tetroxide is easily available as it is already present in institutions with an EM-facility. A downside of using osmium tetroxide is that staining of tissue preserved and/or fixed in alcohol does not work well and osmium tetroxide has limited tissue penetration. For instance, it may already reach an upper penetration limit in specimens that are larger than a mid-gestation mouse. A mid-gestation mouse (developmental stages E8.5 – E13.5) corresponds to 3 – 6 weeks of human gestation [28], whereas a 6 week old embryo is ~ 3 mm in diameter. [29][30] Furthermore, osmium tetroxide is expensive to purchase and to dispose. [14][17]

Phosphor-acids

Phosphor-acid stains can be subdivided into phosphotungstic acids (PTA) and phosphomolybdic acids (PMA). PMA has the chemical formula $H_3PMo_{12}O_{40}$, the chemical formula of PTA is $H_3PW_{12}O_{40}$. The latter is acidic in solution. Molybdenum (M) in PMA and tungsten (W) in PTA are the elements with the highest atomic numbers that confers strong X-ray contrast when attached to biological tissues. The biological tissues that phosphor-acids binds to are fibrin and collagen, which can be found in connective tissue throughout all animal organs. Soft-tissue structures that are visualized (middle and right of *Figure 2*) using these kinds of stains are a.o. eye lens, liver and heart (more can be found in Table 1). Phosphor-acids are very useful stains, especially PTA, because in practice it shows a wide range of densities in tissue corresponding to different tissue types. [24][31] For example, musculature is demonstrated noticeably in CT images. Phosphor-acids penetrate tissues slowly, but it is far less toxic, stable for at least several months, much simpler to use and will effectively stain alcohol-stored samples. According to Metscher et al. using PTA as stain is difficult when imaging embryos of some species since it binds heavily to yolk. Additionally, cartilage does not stain strongly, but will appear as gaps in volume renderings. Lastly, using an acidic stain such as PTA can lead to decalcification of bone tissue and soft-tissue shrinkage. [14] Even though PMA and PTA staining yield similar imaging quality compared to Lugol's solution, the application of these phosphor-acids is limited due to several shortcomings such as irreversible tissue destruction, high prices and poor tissue penetration. [32]

Polyoxometalates

Polyoxometalates (POMs) represent a group of metals such as vanadium, molybdenum or tungsten which are in their highest oxidation state and bridged by oxide anions. The Wells-Dawson POM is one of most studied phosphotungstate POMs. A controlled removal of one tungsten-oxygen unit from the Wells–Dawson POM structure can be replaced by another metal (for example hafnium (Hf) or zirconium). [33] Based on its binding capacity to collagen, connective tissues and blood, its staining capacity, speed of diffusion and the outcome after tissue staining experiments, Vangrunderbeeck et al. concluded that Wells-Dawson polyoxometalate is a highly suitable staining candidate for non-invasive contrast enhanced CT imaging of soft-tissues, with a similar contrast enhancement as that of PTA. [34] Also, Kerckhofs et al. used Hafnium-based Wells-Dawson polyoxometalate (Hf-POM) for staining of bone (marrow), but noted in addition that the vascular network could be visualized and discriminated from the other tissues as well, allowing full 3D blood vessel network assessment. [33][35] According to Heimel et al., using Hf-POM as a stain can be considered when shrinkage needs to be avoided. However, these stains are rather expensive in their production and stain different structures. [22]

Table 1 *Overview of the stains' binding preferences, visualized soft-tissue structures and the (dis)advantages of Lugol's solution, osmium tetroxide, phosphothugstic acid and phosphomolybdic acid. [24]*

Stain	Binds to	Visualizes	Advantages	Disadvantages
Lugol's solution	Glycogen Carbohydrates Lipids	Nerves, myelinated nervous tissue	Simple staining protocol, minimum tissue shrinkage, cost-effective & non-toxic	Tissue shrinkage if concentration is too high & no specific binding
OsO_4	Lipids Proteins Nucleic acids	Eye lens, liver, heart, lungs, thymus, blood (vessels), metanephros, adrenal gland, nucleus pulposus, epithelia, cell dense brain regions, muscle, cartilage	Electron binding energy favourable for strong X-ray absorption & easily available	Toxic, limited tissue penetration, expensive (to purchase and get rid of) & cannot stain alcohol preserved samples
PTA	Connective tissue (fibrin, collagen)	Eye lens, liver, heart, lungs, thymus, blood (vessels), metanephros, epithelia, glands, cell dense brain regions, muscle, cartilage	Shows a wide range of densities, less toxic, stable for months, simple to use & effective in staining alcohol preserved samples	Slow staining penetration, cartilage will appear as a "volume rendering gap", decalcification of bone, soft-tissue shrinkage & high costs
PMA	Collagen (phospholipids)	Eye retina, liver, lungs, thymus, blood (vessels), metanephros, epithelia, glands, cell dense brain region, muscle, cartilage		
POMs	Collagen Connective tissue Blood Vascular network	Bone, bone marrow and soft-tissue	Avoids shrinkage	Expensive stain and stain different structures

3.2 Staining Protocol

Over the years, various staining protocols are used to enhance μCT contrast. For this section the staining protocols of the ten most relevant publications from PubMed were analysed (see Section 2. Method). An overview of these protocols can be found in Table 2 (Appendix A - Staining Protocols). The table is set up in a such a way that readers can sort/order data from this table and/or use it as a basis to develop new staining protocols. In general, a staining protocol provides information about: fixation, staining and imaging (the latter being beyond the scope of this study).

First, a fixation is necessary for storage of the specimen prior to staining and imaging. Gignac et al. recommend to prepare for fixation the "freshest" possible tissues in order to maximize the quality of the specimens sampled. They also note that the treatment of the specimen (freezing before fixation, fixation choice and process) can influence staining outcomes. [36] Choosing the fixative, different aspects are taken into account like personal preference, costs, availability and potential for specimen shrinkage. Metscher et al. provided a scheme with notes on available fixatives. They added a footnote in which they state that the best fixative for μCT scanning will be the best histological fixative for the particular tissues under investigation. [17] Iodine-based staining can - after ethanol storage - be a problem, since lipids are soluble in alcohols (see also Section 3.1 Stains - Lugol's Solution). [36] In that respect it should be noted that specimen storage in ethanol should be limited.

Secondly, the staining is applied. Just as there are different fixations, there are different stains. The following authors wrote valuable information about using iodine/Lugol's solution as contrast agent: Metscher, de Crespigny, Vickerton, Degenhardt, Heimel, Li, Wong and Hutchinson et al. [2], [3], [14], [18], [20]–[23], [37] PTA was mainly discussed by Metscher, Descamps and Xia et al. [3], [14], [24], [32] Metscher, Descamps, Miko, Scheller and Palade et al. discussed osmium tetroxide. [3], [14], [24]–[27] During the literature study, two other stains were found as well PMA [24] and POMs. POMs is discussed by de Bournonville, Kerckhofs and shortly mentioned by Heimel et al. [22], [33]–[35] Detailed information about the aforementioned stains can be found in Section 3.2 Stains, whereas Table 1 gives an overview of the stains' binding preferences, visualized soft-tissue structures and their (dis)advantages.

Together with the used stain, the staining success also depends on three factors that influence each other: specimen size, staining solution concentration and staining time. Table 2 (Appendix A – Staining Protocols) shows that specimens vary in size from small insects to embryonic chick(s) (limbs) of a few mm, but also (parts of) mice and larger human embryos of a couple of cm were researched. Regarding staining solution concentration, most staining protocols used low concentrations (1 – 5 % stain dissolved in (m)ethanol or water). Higher concentrations were also used, but frequently resulted into tissue shrinkage. Staining times also vary. In general, small specimen are stained for a shorter period of time (a couple hours or overnight) whereas larger specimen are stained for 24 hours up to a couple of days.

Conclusion

In conclusion, a μCT scanning staining protocol for (human) foetal imaging consists out of three steps: fixation, staining and imaging. Fixation is necessary for storage and it is recommended to fix the tissue as "fresh" as possible to maximize specimen quality. An important remark is to be careful with an ethanol fixation because lipids are soluble in alcohols. With regards to staining, there are lots of different stains available, of which Lugol's solution, osmium tetroxide and PTA are the most familiar and PMA and Hf-POMs are less commonly known. Of these stains, Lugol's solution is most commonly used as it has a simple staining protocol and is cost-effective, reversible and nontoxic. A downside of using Lugol's solution is the concentration-dependent tissue shrinkage. However, literature suggests that if a concentration of 3.75% (at the most) is used, tissue shrinkage can be prevented. Osmium tetroxide is described as being easily available, but the high costs, toxicity and limited tissue penetration make it less suitable. On the other hand, PTA and PMA show wide ranges of densities and are less toxic compared to osmium tetroxide, but their slow staining penetration and soft-tissue shrinkage also lower the chance of using it as a contrast agent. Lastly, Hf-POMs avoid tissue shrinkage but is expensive compared to Lugol's solution. Weighing the positives against the negatives, the best option is using Lugol's solution as a stain.

In the end, staining success depends on three factors that influence each other: specimen size, used staining solution concentration and staining time. To get better insight into their successes, these factors should be researched individually. Therefore, calculations on staining speed and objectively assessing staining homogeneity are suggested for further research. The combination of the successes found will thereafter lead to the "most optimal" staining protocol for post-mortem (human) foetal μCT imaging.

References

[1] B. S. De Bakker et al., "An interactive three-dimensional digital atlas and quantitative database of human development," Science (80-.)., vol. 354, no. 6315, 2016, doi: 10.1126/science.aag0053.

[2] K. Degenhardt, A. C. Wright, D. Horng, A. Padmanabhan, and J. A. Epstein, "Rapid 3D phenotyping of cardiovascular development in mouse embryos by micro-CT with iodine staining," Circ. Cardiovasc. Imaging, vol. 3, no. 3, pp. 314–322, 2010, doi: 10.1161/CIRCIMAGING.109.918482.

[3] B. D. Metscher and G. B. Müller, "MicroCT for molecular imaging: Quantitative visualization of complete three-dimensional distributions of gene products in embryonic limbs," Dev. Dyn., vol. 240, no.

10, pp. 2301–2308, 2011, doi: 10.1002/dvdy.22733.
[4] Y. Dawood, G. J. Strijkers, J. Limpens, R. J. Oostra, and B. S. de Bakker, “Novel imaging techniques to study postmortem human fetal anatomy: a systematic review on microfocus-CT and ultra-high-field MRI,” Eur. Radiol., vol. 30, no. 4, pp. 2280–2292, 2020, doi: 10.1007/s00330-019-06543-8.
[5] M. C. Goorden, “Lecture Medical Imaging Signals and Systems ‘Conventional X-Ray and CT,’” 2020.
[6] P. Suetens, Fundamentals of Medical Imaging, Second Edi. Cambridge University Press, 2009.
[7] S. Cheriyedath, “Micro-CT Principles, Strengths, and Weaknesses,” 26-2-2019. [Online]. Available: https://www.news-medical.net/life-sciences/Micro-CT-Principles-Strengths-and-Weaknesses.aspx.
[8] J. C. Hutchinson, S. C. Shelmerdine, I. C. Simcock, N. J. Sebire, and O. J. Arthurs, “Early clinical applications for imaging at microscopic detail: Microfocus computed tomography (micro-CT),” Br. J. Radiol., vol. 90, no. 1075, pp. 1–10, 2017, doi: 10.1259/bjr.20170113.
[9] G. R. Choppin, “Absorption of Nuclear Radiation,” in Radiochemistry & Nuclear Chemistry, Elsevier Inc., 2013, pp. 163–208.
[10] H.-J. B. and L. M. Freeman, Clinical Nuclear Medicine. 2007.
[11] T. Alexeev, B. Kavanagh, M. Miften, and C. Altunbas, “Two-dimensional antiscatter grid: A novel scatter rejection device for Cone-beam computed tomography: A,” Med. Phys., vol. 45, no. 2, pp. 529–534, 2018, doi: 10.1002/mp.12724.
[12] AAPM, “Tomographic Image Reconstruction.” [Online]. Available: https://www.aapm.org/meetings/99AM/pdf/2806-57576.pdf.
[13] S. W. Smith, Digital Signal Processing. 2003.
[14] B. D. Metscher, “MicroCT for developmental biology: A versatile tool for high-contrast 3D imaging at histological resolutions,” Dev. Dyn., vol. 238, no. 3, pp. 632–640, 2009, doi: 10.1002/dvdy.21857.
[15] L. Hrvoje and M. W. Greenstaff, X-Ray Computed Tomography Contrast Agents, vol. 113, no. 3. 2014.
[16] J. K. Shultis and R. E. Faw, Fundamentals of Nuclear Science and Engineering, Second Edi. 2007.
[17] B. D. Metscher, “Micro CT for comparative morphology: Simple staining methods allow high-contrast 3D imaging of diverse non-mineralized animal tissues,” BMC Physiol., vol. 9, no. 1, 2009, doi: 10.1186/1472-6793-9-11.
[18] P. Vickerton, J. Jarvis, and N. Jeffery, “Concentration-dependent specimen shrinkage in iodine-enhanced microCT,” J. Anat., vol. 223, no. 2, pp. 185–193, 2013, doi: 10.1111/joa.12068.
[19] Y. Dawood and B. S. de Bakker, “Micro-CT of early human development,” Radiology, vol. 297, no. 1, p. 32, 2020, doi: 10.1148/radiol.2020201660.
[20] A. de Crespigny, H. Bou-Reslan, M. C. Nishimura, H. Phillips, R. A. D. Carano, and H. E. D’Arceuil, “3D micro-CT imaging of the postmortem brain,” J. Neurosci. Methods, vol. 171, no. 2, pp. 207–213, 2008, doi: 10.1016/j.jneumeth.2008.03.006.
[21] J. C. Hutchinson et al., “Postmortem microfocus computed tomography for early gestation fetuses: a validation study against conventional autopsy,” Am. J. Obstet. Gynecol., vol. 218, no. 4, pp. 445.e1-445.e12, 2018, doi: 10.1016/j.ajog.2018.01.040.
[22] P. Heimel et al., “Iodine-enhanced micro-CT imaging of soft tissue on the example of peripheral nerve regeneration,” bioRxiv, vol. 2019, 2018, doi: 10.1101/477539.
[23] Z. Li, J. A. Clarke, R. A. Ketcham, M. W. Colbert, and F. Yan, “An investigation of the efficacy and mechanism of contrast-enhanced X-ray Computed Tomography utilizing iodine for large specimens through experimental and simulation approaches,” BMC Physiol., vol. 15, no. 1, pp. 1–16, 2015, doi: 10.1186/s12899-015-0019-3.
[24] E. Descamps, A. Sochacka, B. de Kegel, D. Van Loo, L. Hoorebeke, and D. Adriaens, “Soft tissue discrimination with contrast agents using micro-ct scanning,” Belgian J. Zool., vol. 144, no. 1, pp. 20–40, 2014, doi: 10.26496/bjz.2014.63.
[25] G. E. PALADE, “A study of fixation for electron microscopy.,” J. Exp. Med., vol. 95, no. 3, pp. 285–298, 1952, doi: 10.1084/jem.95.3.285.
[26] E. L. Scheller et al., “Use of osmium tetroxide staining with microcomputerized tomography to visualize and quantify bone marrow adipose tissue in vivo,” Methods Enzymol., vol. 537, pp. 123–139, 2014, doi: 10.1016/B978-0-12-411619-1.00007-0.
[27] M. Miko, “Histologic Examination of Peripheral Nerves,” in Nerves and Nerve Injuries, 2015, pp. 79–89.
[28] S. Srinivasan et al., “Noninvasive, in utero imaging of mouse embryonic heart development with 40-MHz echocardiography,” Circulation, vol. 98, no. 9, pp. 912–918, 1998, doi: 10.1161/01.CIR.98.9.912.

[29] Elaine N. Marieb & Katja Hoehn, Human Anatomy & Physiology, 10th Editi. 2016.
[30] Y. Dawood, “Human gestation,” 2021.
[31] MicroPhotonics, “Ex vivo staining of embryos (mouse) with phosphotungstic acid for soft tissue contrast in micro-CT imaging.” [Online]. Available: https://www.microphotonics.com/assets/base/doc/embryostainingwithPTAforexvivomicro-ctimaging.pdf.
[32] C. W. Xia et al., “Lugol’s Iodine-Enhanced Micro-CT: A Potential 3-D Imaging Method for Detecting Tongue Squamous Cell Carcinoma Specimens in Surgery,” Front. Oncol., vol. 10, no. October, pp. 1–10, 2020, doi: 10.3389/fonc.2020.550171.
[33] S. de Bournonville et al., “Exploring polyoxometalates as non-destructive staining agents for contrast-enhanced microfocus computed tomography of biological tissues,” Acta Biomater., vol. 105, no. January, pp. 253–262, 2020, doi: 10.1016/j.actbio.2020.01.038.
[34] S. De Bournonville, S. Vangrunderbeeck, and G. Kerckhofs, “Contrast-enhanced microCT for virtual 3D anatomical pathology of biological tissues: A literature review,” Contrast Media Mol. Imaging, vol. 2019, pp. 5–6, 2019, doi: 10.1155/2019/8617406.
[35] G. Kerckhofs et al., “Simultaneous three-dimensional visualization of mineralized and soft skeletal tissues by a novel microCT contrast agent with polyoxometalate structure,” Biomaterials, vol. 159, pp. 1–12, 2018, doi: 10.1016/j.biomaterials.2017.12.016.
[36] P. M. Gignac et al., “Diffusible iodine-based contrast-enhanced computed tomography (diceCT): An emerging tool for rapid, high-resolution, 3-D imaging of metazoan soft tissues,” J. Anat., vol. 228, no. 6, pp. 889–909, 2016, doi: 10.1111/joa.12449.
[37] M. D. Wong, S. Spring, and R. M. Henkelman, “Structural stabilization of tissue for embryo phenotyping using micro-CT with iodine staining,” PLoS One, vol. 8, no. 12, pp. 1–7, 2013, doi: 10.1371/journal.pone.0084321.

List of Figures

List of Tables

Appendix A – Staining Protocols

Table 2 *An overview of literature that uses different approaches. Information about the embryo/foetus, staining solutions, their specifications and staining times found in published literature.*

Staining Protocols						
First Author	**Year of Publication**	**Title**	**Embryo/Foetus**	**Staining**	**Specifications**	**Staining time**
de Crespigny	2008	3D micro-CT imaging of the postmortem brain	Rabbits Mice	Iodine	Perfusion fixed with 4% paraformaldehyde	5 d.
					1: Pure phosphate buffered saline solution (PBS)	5 d.
					2: Iodinated contrast (Diatrizoate Meglumine and Diatrizoate Sodium), diluted 1:20, 1:10 or 1:5 with PBS, resulting in I-127 concentrations of 0.14, 0.27 and 0.49 M respectively	5 d.
Brian D. Metscher	2009a	MicroCT for comparative morphology: simple staining methods allow high-contrast 3D imaging of diverse non-mineralized animal tissues	Animal soft-tissues (vertebrates, mouse embryos, insects and other invertebrates)	PTA (1% (w/v) phosphotungstic acid in water)	Mix 30 ml 1% PTA solution + 70 ml absolute ethanol to make 0.3% PTA in 70% ethanol. Keeps indefinitely. Take samples to 70% ethanol. Change to 70% ethanol. Staining is stable for months. Scan samples in 70 - 100% ethanol.	Overnight (or longer)
				I_2KI (1% iodine metal (I_2) + 2% potassium iodide (KI) in water)	Dilute to 10% in water just before use. Rinse samples in water. Wash in water. Can be scanned in water or dehydrated to alcohol.	Overnight
				I_2E, I_2M (1% iodine metal (I_2) dissolved in 100% ethanol (I_2E) or methanol (I_2M)	Use at full concentration or dilute in absolute alcohol. Take samples to 100% alcohol. Stain overnight (or longer). Wash in alcohol. Stain does not need to be completely washed out before scanning.	Overnight (or longer)
				Osmium tetroxide (standard EM post-fixation)	Same as routine EM processing. Osmium-stained samples can be scanned in resin blocks, with some loss of contrast.	?
Brian D. Metscher	2009b	MicroCT for Developmental Biology: A Versatile Tool for High-Contrast 3D Imaging at Histological Resolutions	Chicks	5% Gallocyanin-chromalum in water 1% iodine in ethanol 10% IKI 0.3% PTA in 70% ethanol Osmium tetroxide	Each stain was washed out with its respective solvent, and all samples were dehydrated to ethanol.	Overnight

Karl Degenhardt	2010	Rapid 3D Phenotyping of Cardiovascular Development in Mouse Embryos by Micro-CT With Iodine Staining	Mice	Lugol's solution	10 g KI + 5 g I_2 in 100 mL water 986 mmol/L iodine 1204 mOsm/L osmolarity	24, 48 and 72 h.
Brain D. Metscher	2011	MicroCT for Molecular Imaging: Quantitative Visualization of Complete Three-Dimensional Distributions of Gene Products in Embryonic Limbs	Chicks (embryonic limbs)	Immunostaining with peroxidase-conjugated secondary antibodies	Glyoxal-based fixative	2 - 3 h.
					Rinse samples in methanol	
					3% hydrogen peroxide	30 m.
					Rehydration trough methanol series (75%, 50%, 25%, 10 min. each) to MABT (100 mM maleic acid, 150 mM NaCl, 0.1% Trition X-100, pH 7.4)	10 m. each
					Wash samples in MABT + 0.1% saponin, blocked in a blocking solution (MABT with 0.1% saponin, 10% sheep serum, 0.5% Roche Blocking Reagent and 1% dimethylsulfoxide)	10 m. in MABT, 1 h. to block
					Incubate	Overnight (or longer)
					Wash excess antibodies with 5 (or more) washes in MABT (with 1 wash left overnight)	
					Postfixed samples in 10% formalin in MABT, washed 3x in double distilled H_2O. 0.1% Triton X-100 in double distilled H_2O	20 min. in MABT, 3x 10 m. each
				X-ray constrasting of immonoprobe with an enzyme-mediated silver precipitation scheme	Enzyme metallography kit: Nanoprobes EnzMet 6010 from Nanoprobes Inc. (Yaphank, NY)	
					300 μL of Solution B was added and mixed, after 300 μL of Solution C was added and mixed	Sol. B 4 m., Sol. C 5 - 20 m.
					Change to 1% sodium thiosulfate in 0.1% Triton	10 m.
					Rinse samples in distilled water	5 m.
					Change to 75% methanol followed by 100% methanol	
Vickerton	2013	Concentration-dependent specimen shrinkage in iodine-enhanced microCT	Mice (skeletal muscle, cardiac muscle and cerebellum)	Lugol's solution	Immersed in 10 % formaldehyde in PBS 3% gluteraldehyde in PBS 70% ethanol or solutions of 2, 6, 10 and 20% Lugol's solution, dissolved in 10% PBFS (F stands for formalin)	Volume measurements after 1, 2, 7, 14 and 28 d.

Wong	2013	Structural Stabilization of Tissue for Embryo Phenotyping Using Micro-CT with Iodine Staining	Mice	Lugol's solution	Mouse embryos are placed in phosphate buffered saline (PBS) solution	
					Fixation in 4% paraformaldehyde	Overnight
					Stored in PBS	
					Protocol A: samples immersed in 0.025 N Lugol's solution	24 h.
					Protocol B: samples stabilized with hydrogel treatment and immersed in 0.025 N Lugol's solution	3 d.
					Protocol C: samples immersed in 0.1 N Lugol's solution	72 h.
					Protocol D: samples stabilized with hydrogel treatment and immersed in 0.1 N Lugol's solution	3 d.
					Staining solutions are replaced every 8 h.	
Kerckhofs	2016	Novel non-invasive contrast agents for virtual histology and 3D quantification of soft tissues	Mice (femur, kidney)	Hf-POM	Harvest and fixation in paraformaldehyde	
					Stained with PTA (3.5 %)	24 h.
					Stained with Hf-POT (3.5 %)	24 h.
Hutchinson	2018	Postmortem microfocus computed tomography for early gestation fetusus: a validation study against conventional autopsy	Humans	Lugol's solution	10% formalin + I_2KI/Lugol's solution	
					Iodine content: 63.25 mg/mL in a 1:1 ratio	72 h.
					Rinsed in water	
					Dried with gauze	
Dawood	2019	Novel imaging techniques to study post-mortem human fetal anatomy: a systematic review on microfocus-CT and ultra-high-field MRI	Humans	Lugol's solution	Fixation in 4% paraformaldehyde	
					Staining by 3.75% (w/v) Lugol's solution	48 h. to 7 d.
					Washing of redundant Lugol's solution with water	1 h.
Heimel	2019	Iodine-Enhanced Micro-CT Imaging of Soft Tissue on the Example of Peripheral Nerve Regeneration	Mice (for- and hindlimbs) Rat (organ- and tissue samples)	Lugol's solution	One part iodine + two parts potassium iodide in anqueous solution (0.3% or 0.1% w/v iodine and 0.2% w/v potassium iodide) in double distilled H_2O	24 h.

Appendix II – Ethics: Patient Information Form (Dutch Only)

Amsterdam, januari 2020

Informatie over wetenschappelijk onderzoek naar Down syndroom

Geachte mevrouw,

Met deze brief willen wij u informeren over een wetenschappelijk onderzoek waarvoor wij uw medewerking willen vragen.

U heeft besloten uw zwangerschap af te breken. Wij zijn ons ervan bewust dat dit voor u een bijzonder emotionele beslissing is. We begrijpen ook dat dit een moeilijk moment is om benaderd te worden met de vraag om mee te doen aan wetenschappelijk onderzoek. Wij willen op voorhand benadrukken dat u helemaal vrij bent om al of niet uw medewerking te verlenen aan het onderzoek. Het gaat om een onderzoek naar Down syndroom. Voor dit onderzoek is goedkeuring verkregen van de medisch ethische toetsingscommissie van het AMC.

Doel van het onderzoek
In dit onderzoek willen wij meer te weten komen over hoe het komt dat iemand die drie in plaats van twee chromosomen 21 heeft, de kenmerken krijgt die we Down syndroom noemen. Als we weten hoe dit komt, kunnen we ook beter begrijpen waarom iemand met Down syndroom een probleem krijgt aan bijvoorbeeld het hart of de hersenen.
We willen bij het onderzoek naar alle organen en weefsels kijken, ook naar de placenta. Dus niet alleen naar het hart of de hersenen maar ook de long, de darm, de huid, de spieren enz. In feite zal onderzoek gedaan worden met alle weefsels.
We willen één onderzoek hier apart noemen: soms zullen we bijvoorbeeld hartcellen of levercellen zo veranderen, dat deze langer (weken of zelfs maanden) blijven groeien. Cellen die groeien laten kenmerken zien die we in niet-delende cellen niet kunnen zien. Daardoor geven ze een schat aan informatie aan onderzoekers.

Plaats van het onderzoek
Alle onderzoek vindt plaats binnen het AMC. Via een MRI of CT scan kunnen we precies de bouw van alle weefsel zichtbaar maken. Het weefsel en de MRI/CT beelden worden opgeslagen in een biobank. De opslag van het weefsel is op een centrale plaats, maar het onderzoek zelf gebeurt vooral door artsen die gespecialiseerd zijn in onderzoek van een orgaan zoals een (kinder)cardioloog of een (kinder)neuroloog. Als onderzoekers uit andere universiteiten uit binnenland of buitenland vragen of ze ook gebruik mogen maken van de weefsels, zullen we als het kan dat toestaan: we willen dat alle weefsels zoveel mogelijk gebruikt worden. Ze kunnen het dan doen zonder daarvoor te betalen. Onderzoek door bedrijven of andere commerciële instellingen zijn niet toegestaan.

Duur van het onderzoek
Alle weefsels zullen lang bewaard worden: 50 jaar. Reden is dat het kostbaar weefsel is en we er zoveel mogelijk gebruik van willen maken. Door het zo lang te bewaren zal waarschijnlijk elk weefsel van elk orgaan uiteindelijk helemaal opgebruikt kunnen worden.

Vrijwillige medewerking
U bent helemaal vrij om mee te doen aan dit onderzoek of niet. Als u niet wilt meedoen, hoeft u daarvoor geen reden te geven. Uw besluit zal geen enkele verandering brengen in uw zorg of begeleiding.

Proefpersonen informatie
versie 4.4
datum 27.01.2020

Als u nu toestemming geeft, kunt u tot vlak na de ingreep uw toestemming weer intrekken. Ook daarvoor hoeft u geen reden te geven. Als u op een later tijdstip uw toestemming zou willen intrekken, is dat niet meer mogelijk: we slaan alle weefsels anoniem op, dus zonder enig gegeven erbij waaraan te zien zou zijn dat het van u afkomstig is. We kunnen het weefsel dan niet meer achterhalen.

Bescherming van privacy

Aangezien het weefsel van de foetus anoniem bewaard wordt, zal uw persoonlijke privacy gewaarborgd zijn. Als u toestemt mee te doen, wordt u verzocht een toestemmingsformulier in te vullen en te ondertekenen. Dit formulier zal in het (beveiligde) archief van de biobank bewaard worden als bewijs van uw toestemming. Op dit formulier staan wel uw persoonlijke gegevens. Maar het foetale weefsel en deze persoonsgegevens zullen niet tot elkaar herleid kunnen worden.

Natuurlijk zullen we alle regels die gelden voor opslag van menselijk materiaal nauwkeurig volgen. Die regels staan vermeld in een apart reglement. Als u wilt kunt u dit reglement (“Fetal Aneuploidy Biobank”) inzien of er een kopie van krijgen. U kunt dit aan de hoofdonderzoeker, dr. de Bakker, vragen (b.s.debakker@amc.uva.nl of 06 50063079). Zoals altijd is er toezicht op onze manier van werken. Dat kan gebeuren door vertegenwoordigers van het AMC die opdracht tot het onderzoek gaf, en vertegenwoordigers van de inspectie voor de gezondheidszorg.

Meer vragen

Als u na het lezen van deze informatiebrief en het bespreken ervan met de arts, nog vragen hebt, kunt u altijd contact opnemen met de hoofdonderzoeker, dr. de Bakker. Als u liever wilt overleggen met een arts die niet bij het onderzoek betrokken is maar wel weet wat het onderzoek inhoudt, kunt u contact opnemen met mevr. Drs. S. Maas, klinisch geneticus (s.m.maas@amc.uva.nl of 020 5668844).

We wensen u sterkte toe in deze voor u emotionele periode.

Met vriendelijke groet,

Dr Bernadette S De Bakker
Klinisch embryoloog

Proefpersonen informatie
versie 4.4
datum 27.01.2020

Bijlage I
Informatie over wetenschappelijk onderzoek naar Down syndroom

Toestemmingsformulier wetenschappelijk onderzoek

Toestemmingsverklaring voor het afstaan van foetaal weefsel ten behoeve van het wetenschappelijk onderzoek naar Down syndroom

Datum en tijdstip* van besluit tot abortus: . . . . . .

Datum en tijdstip* van informatie over wetenschappelijk onderzoek: . . . . . .

Ik ben naar tevredenheid over het onderzoek geïnformeerd. Ik heb de schriftelijke informatie gelezen en heb vragen kunnen stellen over het onderzoek. Mijn vragen zijn naar tevredenheid beantwoord. Ik heb voldoende tijd gehad om over mijn medewerking aan het onderzoek te kunnen nadenken. Ik weet dat ik mijn toestemming weer kan intrekken zonder dat ik daarvoor een reden hoef te geven. Ik weet dat de tijd voor het intrekken van mijn toestemming beperkt is, omdat het weefsel anoniem bewaard en gebruikt zal worden, en het dan niet meer te achterhalen is.

Ik geef vrijwillig toestemming voor deelname aan het onderzoek.

Naam: . . . . . .

Plaats: . . . . . .

Handtekening: . . . . . .

Datum en tijdstip*: . . . . . .

* De tijdstippen van het abortusbesluit, van het krijgen van informatie en het geven van toestemming zijn van belang omdat duidelijk moet zijn dat het besluit tot abortus is genomen vóórdat informatie is gegeven over het wetenschappelijk onderzoek en vóórdat daarvoor toestemming is gevraagd.

Proefpersonen informatie
versie 4.4
datum 27.01.2020

Bijlage II
Informatie over wetenschappelijk onderzoek naar Down syndroom

Intrekkingsformulier

Hierbij trek ik mijn op (….datum) gegeven toestemming voor het gebruik van foetaal weefsel ten behoeve van het wetenschappelijk onderzoek naar Down syndroom in en ik verzoek dit weefsel te vernietigen.

Ik begrijp dat alleen tot opslag het weefsel te achterhalen is en daarna niet meer; foetaal weefsel dat al anoniem is opgeslagen, kan niet meer worden vernietigd.

Naam: ……

Handtekening: ……..……

Datum: ……..

Proefpersonen informatie
versie 4.4
datum 27.01.2020

Appendix III – Buffers

Sörensen's Buffer (2x)

Prepare stock solutions and combine prior to use to achieve desired pH values (see *Table 3*).

266 mM Na_2HPO_4 72.52 g. $Na_2HPO_4.5H_2O$ in 1L Milli-Q water
266 mM KH_2PO_4 18.16 g. KH_2PO_4 in 1L Milli-Q water

Table 3 *Sörensen's Buffer*

pH	mL Na_2HPO_4	mL KH_2PO_4
5.0	1.0	99.0
5.2	2.0	98.0
5.4	3.0	97.0
5.6	5.0	95.0
5.8	7.8	92.2
6.0	12.0	88.0
6.2	18.5	81.5
6.4	26.5	73.5
6.6	37.5	62.5
7.0	50.0	50.0
7.2	71.5	28.5
7.4	80.4	19.6
7.6	86.8	13.2
7.8	91.4	8.6
8.0	94.5	5.5
8.2	96.5	3.5

Citrate Buffer (2x)

Table 4 shows different pH values for citrate buffer.

Table 4 *Citrate Buffer*

pH	x mL 0.2 M-citric acid	y mL 0.4-Na_2HPO_4
2.6	89.10	10.90
2.8	84.15	15.85
3.0	79.45	20.55
3.2	75.30	24.70
3.4	71.50	28.50
3.6	67.80	32.20
3.8	64.50	35.50
4.0	61.45	38.55
4.2	58.60	41.40
4.4	55.90	44.10
4.6	53.25	46.75
4.8	50.70	49.30
5.0	48.50	51.50

pH	x mL 0.2 M-citric acid	y mL 0.4-Na_2HPO_4
5.2	46.40	53.60
5.4	44.25	55.75
5.6	42.00	58.00
5.8	39.55	60.45
6.0	36.85	63.15
6.2	33.90	66.10
6.4	30.75	69.25
6.6	27.25	72.75
6.8	22.75	77.25
7.0	17.65	82.35
7.2	13.05	86.95
7.4	9.15	90.85
7.6	6.35	93.65

Appendix IV – Example Fill in Sheet

An example of a fill in sheet (*Table 5*) to write down pH measurements result for different solutions. It is important to write down the date and time of the performed measurements and the measurement timing.

In this example, T0 is the "blanc measurement". The blanc measurement is always performed before the actual measurements begin, so the initial value is known. Then, after a certain amount of time has passed (in this example two hours), the first measurement is performed (T1). Thereafter, frequent measurements are recommended.

Table 5 *Example Fill in Sheet*

pH	**Date**					
	Time					
Conditions		**Label**	**T0**	**T1**	**T2**	**…**
			0	**2**	**4**	
S		S1				
		S0.5				
		S0.25				
SB-Lugol		SB1				
		SB0.5				
		SB0.25				
Citrate (pH = 7)		C7-1				
		C7-0.5				
		C7-0.25				
Citrate (pH = 5)		C5-1				
		C5-0.5				
		C5-0.25				
Citrate (pH = 3)		C3-1				
		C3-0.5				
		C3-0.25				
Citrate with Lugol (pH = 7)		CB7-1				
		CB7-0.5				
		CB7-0.25				
Citrate with Lugol (pH = 5)		CB5-1				
		CB5-0.5				
		CB5-0.25				
Citrate with Lugol (pH = 3)		CB3-1				
		CB3-0.5				
		CB3-0.25				
3.75% Lugol		1				

Appendix V – Solutions without Tissue

In this appendix the different solutions (*Table 6*) and the osmolarity and OD test results (*Figure 26* and *Figure 27*) are presented.

Table 6 *Solutions without Tissue: Scheme of coding (colour and number), a description of the used solutions and the content of the Falcon tubes.*

Colour & Number	Colour coding	Solution Description	Falcon Tube Content [50 mL total volume]								
			7.5% Lugol [mL]	2x SB [mL]	2x C7 [mL]	2x C5 [mL]	2x C3 [mL]	1x C7 [mL]	1x C5 [mL]	1x C3 [mL]	Milli-Q [mL]
1	S1	Sorensens without Lugol 1x buffer		25							25
2	S0.5	Sorensens without Lugol 0.5x buffer		12.5							37.5
3	S0.25	Sorensens without Lugol 0.25x buffer		6.25							43.75
4	SB1	Sorensens with Lugol 1x buffer	25	25							0
5	SB0.5	Sorensens with Lugol 0.5x buffer	25	12.5							12.5
6	SB0.25	Sorensens with Lugol 0.25x buffer	25	6.25							18.75
7	C7-1	Citrate without Lugol pH = 7 1x buffer						50			0
8	C7-0.5	Citrate without Lugol pH = 7 0.5x buffer						25			25
9	C7-0.25	Citrate without Lugol pH = 7 0.25x buffer						12.5			37.5
10	C5-1	Citrate without Lugol pH = 5 1x buffer							50		0
11	C5-0.5	Citrate without Lugol pH = 5 0.5x buffer							25		25
12	C5-0.25	Citrate without Lugol pH = 5 0.25x buffer							12.5		37.5
13	C3-1	Citrate without Lugol pH = 3 1x buffer								50	0
14	C3-0.5	Citrate without Lugol pH = 3 0.5x buffer								25	25
15	C3-0.25	Citrate without Lugol pH = 3 0.25x buffer								12.5	37.5
16	CB7-1	Citrate with Lugol pH = 7 1x buffer	25		25						0
17	CB7-0.5	Citrate with Lugol pH = 7 0.5x buffer	25		12.5						12,5
18	CB7-0.25	Citrate with Lugol pH = 7 0.25x buffer	25		6.25						18.75
19	CB5-1	Citrate with Lugol pH = 5 1x buffer	25			25					0
20	CB5-0.5	Citrate with Lugol pH = 5 0.5x buffer	25			12.5					12.5
21	CB5-0.25	Citrate with Lugol pH = 5 0.25x buffer	25			6.25					18.75
22	CB3-1	Citrate with Lugol pH = 3 1x buffer	25				25				0
23	CB3-0.5	Citrate with Lugol pH = 3 0.5x buffer	25				12.5				12.5
24	CB3-0.25	Citrate with Lugol pH = 3 0.25x buffer	25				6.25				18.75
25	3.75% Lugol	3.75% Lugol	25								25

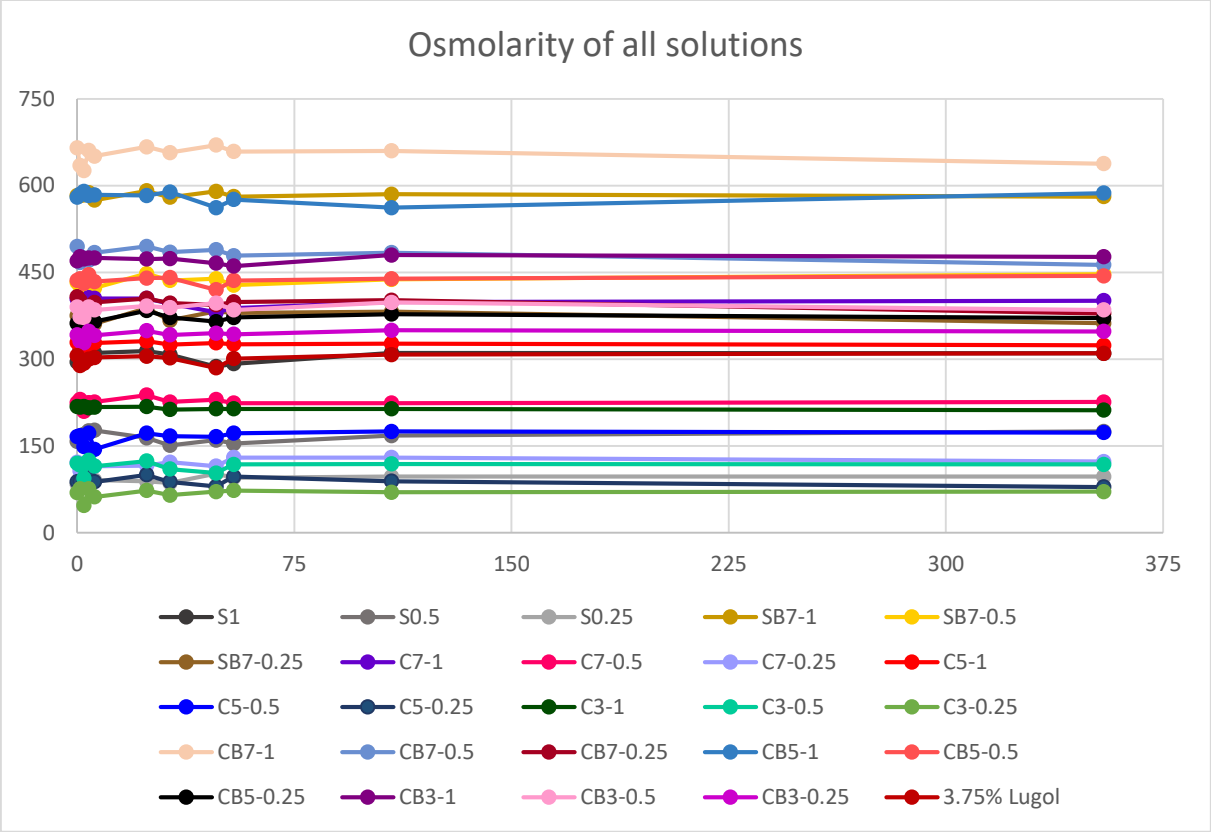

Figure 26 *Osmolarity measurement results (over time) of the solutions without tissue.*

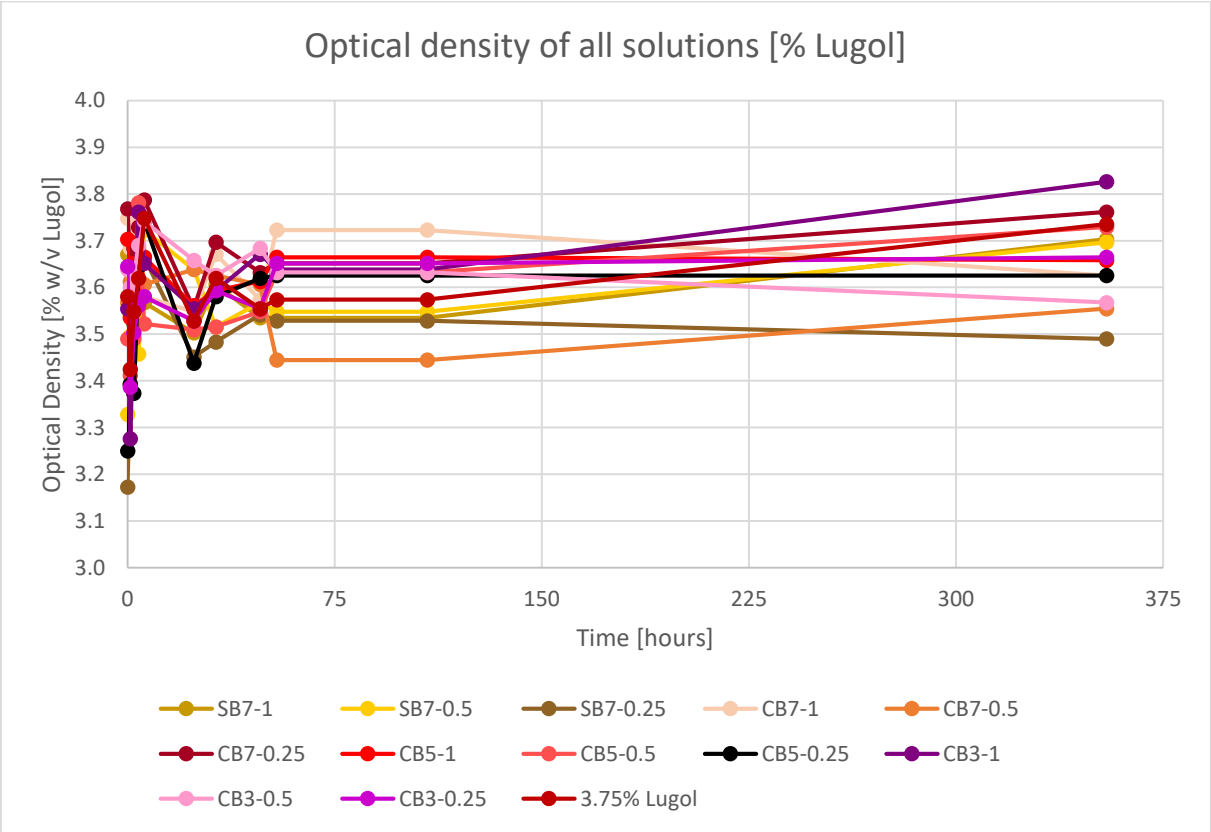

Figure 27 *Optical density measurement results (over time) of the solutions without tissue, expressed in percentages Lugol's solution present in the solution.*

Appendix VI – Pork Liver Tissue Test

In this appendix the different solutions (*Table 7*) used for the pork liver tissue test (AMC method) and their osmolarity, weight, OD and acidity test results are presented (*Figure 28 – Figure 31*). Intensity line profiles of distance/intensity measurements (staining progression) is presented at *page 51 – 53*. The graphs show averages of three pork liver samples (n = 3), immersed in the same solution.

Table 7 *Pork Liver Tissue Test: Scheme of coding (colour and number), a description of the used solutions and the content of the Falcon tubes.*

Colour & Number	Colour coding	Solution Description	Falcon Tube Content [50 mL total volume]						
			7.5% Lugol [mL]	2x SB8 [mL]	2x SB7 [mL]	2x CB7 [mL]	2x CB5 [mL]	2x CB3 [mL]	Milli-Q [mL]
01	SB8-1	Sörensen's Buffered – Lugol (pH = 8)	25	25					
02	SB8-1	Sörensen's Buffered – Lugol (pH = 8)	25	25					
03	SB8-1	Sörensen's Buffered – Lugol (pH = 8)	25	25					
1	SB7-1	Sörensen's Buffered – Lugol (pH = 7)	25		25				
2	SB7-1	Sörensen's Buffered – Lugol (pH = 7)	25		25				
3	SB7-1	Sörensen's Buffered – Lugol (pH = 7)	25		25				
4	CB7-1	Citrate Buffered – Lugol (pH = 7)	25			25			
5	CB7-1	Citrate Buffered – Lugol (pH = 7)	25			25			
6	CB7-1	Citrate Buffered – Lugol (pH = 7)	25			25			
7	CB5-1	Citrate Buffered – Lugol (pH = 5)	25				25		
8	CB5-1	Citrate Buffered – Lugol (pH = 5)	25				25		
9	CB5-1	Citrate Buffered – Lugol (pH = 5)	25				25		
10	CB3-1	Citrate Buffered – Lugol (pH = 3)	25					25	
11	CB3-1	Citrate Buffered – Lugol (pH = 3)	25					25	
12	CB3-1	Citrate Buffered – Lugol (pH = 3)	25					25	
13	3.75% L	3.75% Lugol – without buffer	25						25
14	3.75% L	3.75% Lugol – without buffer	25						25
15	3.75% L	3.75% Lugol – without buffer	25						25
Acidity Test (without Lugol)	CB5-1	Citrate Buffer (pH = 5)					25		25
	CB5-1	Citrate Buffer (pH = 5)					25		25
	CB5-1	Citrate Buffer (pH = 5)					25		25
	CB3-1	Citrate Buffer (pH = 3)						25	25
	CB3-1	Citrate Buffer (pH = 3)						25	25
	CB3-1	Citrate Buffer (pH = 3)						25	25

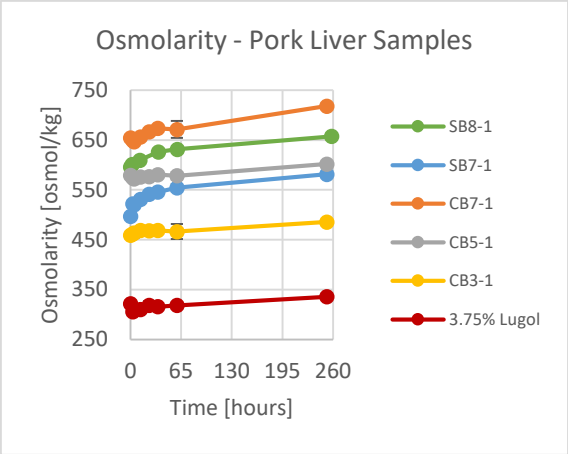

Figure 28 *Averaged osmolarity over time (n = 3).*

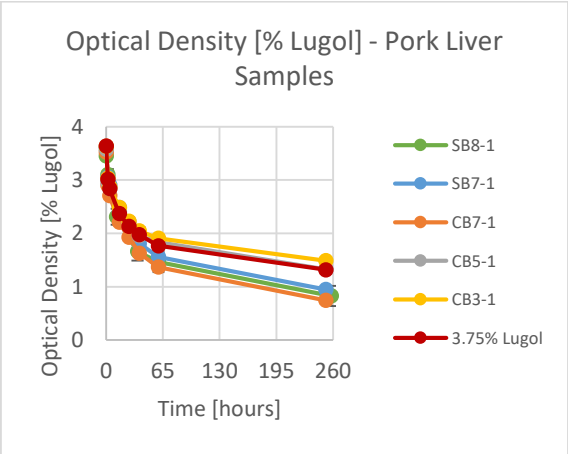

Figure 29 *Averaged optical density over time (n = 3) expressed in percentages Lugol's solution present in the solution.*

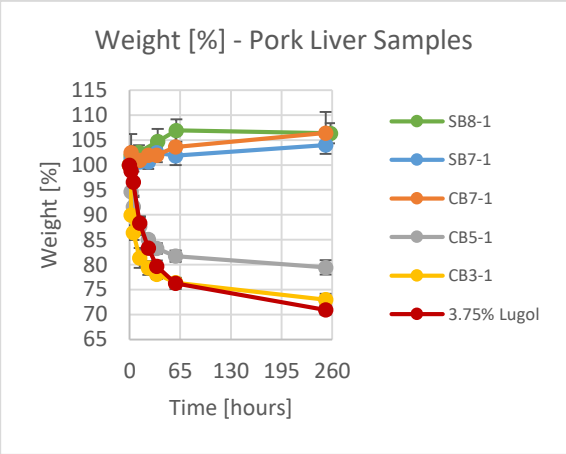

Figure 30 *Averaged weight over time (n = 3) (in percentages) relative to the starting weight.*

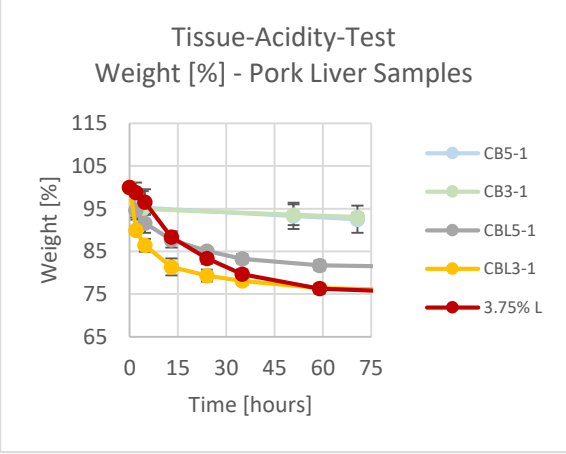

Figure 31 *Tissue-Acidity-Test: Averaged weight over time (n = 3) (in percentages) relative to the starting volume.*

Intensity line profiles of distance/intensity measurements (staining progression):

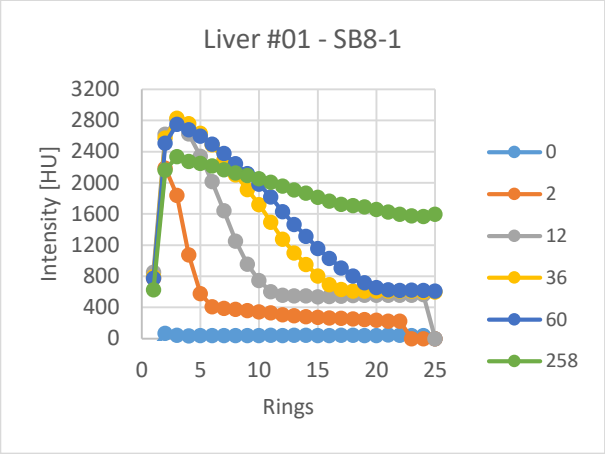

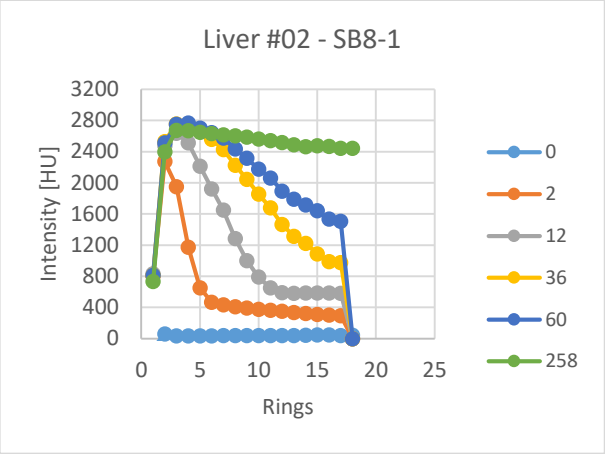

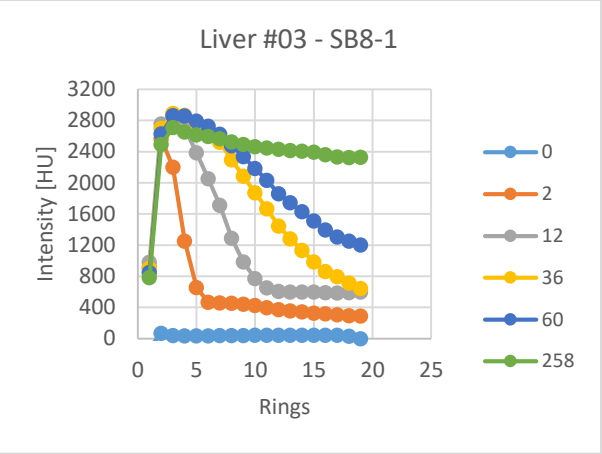

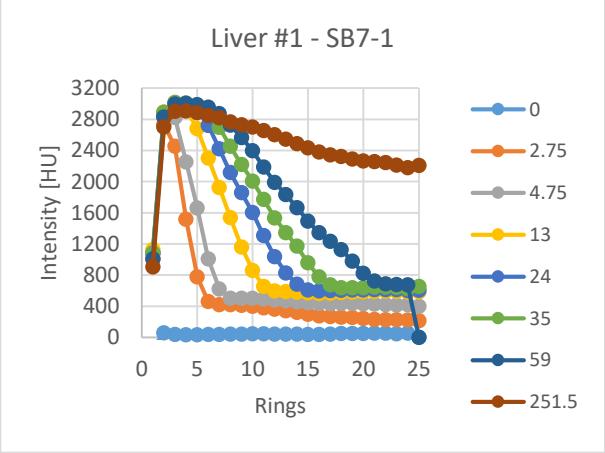

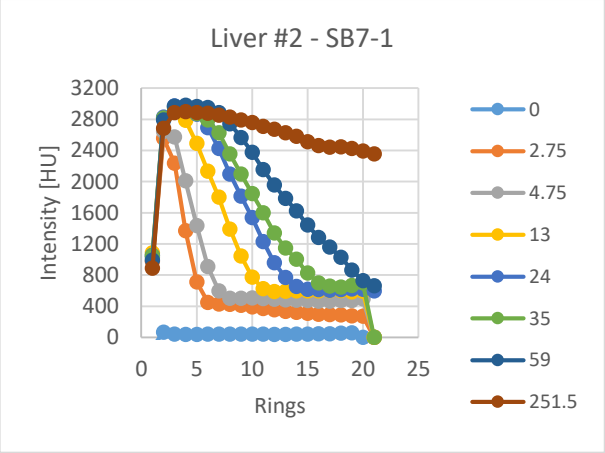

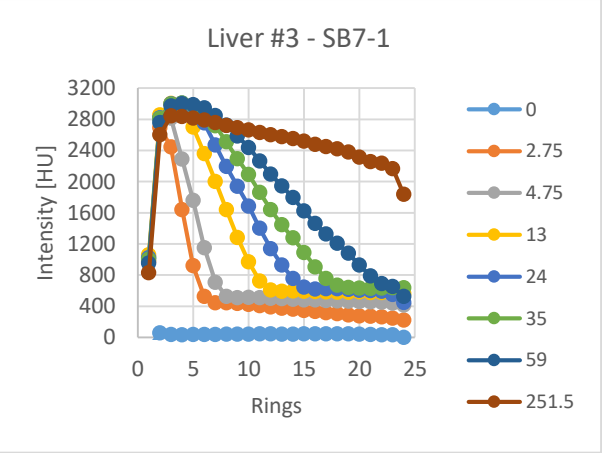

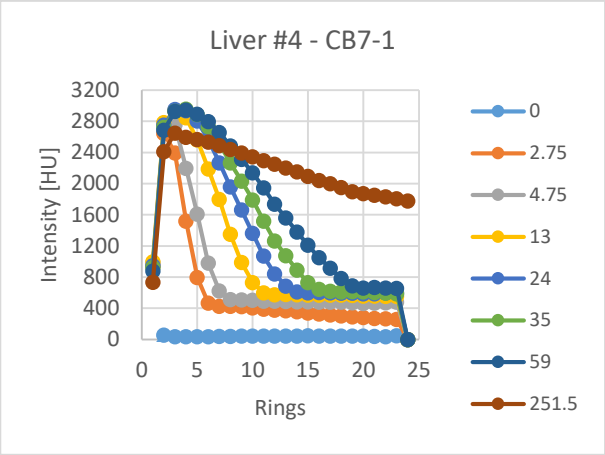
Liver #4 - CB7-1
Intensity [HU]
3200
2800
2400
2000
1600
1200
800
400
0
0 5 10 15 20 25
Rings
0
2.75
4.75
13
24
35
59
251.5

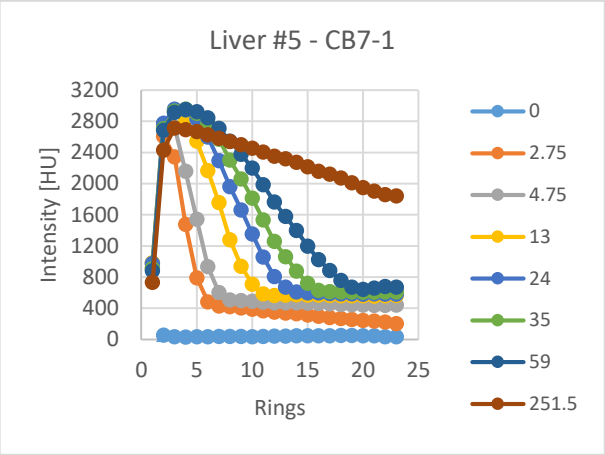
Liver #5 - CB7-1
Intensity [HU]
3200
2800
2400
2000
1600
1200
800
400
0
0 5 10 15 20 25
Rings
0
2.75
4.75
13
24
35
59
251.5

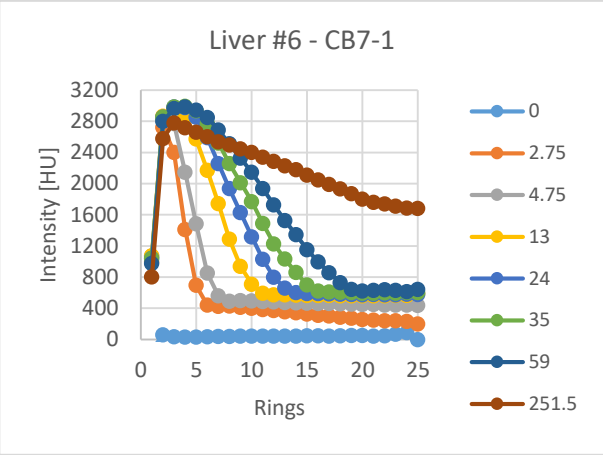
Liver #6 - CB7-1
Intensity [HU]
3200
2800
2400
2000
1600
1200
800
400
0
0 5 10 15 20 25
Rings
0
2.75
4.75
13
24
35
59
251.5

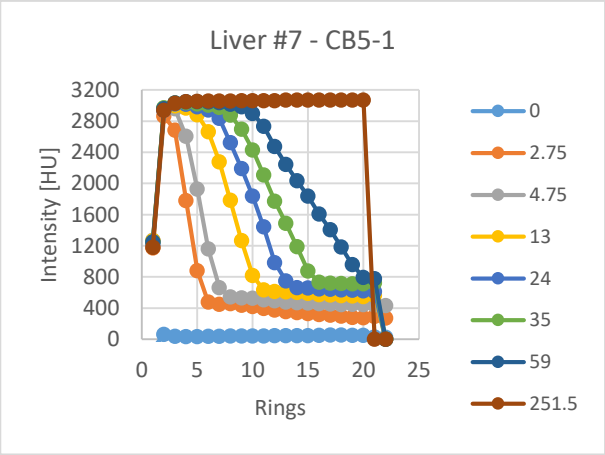
Liver #7 - CB5-1
Intensity [HU]
3200
2800
2400
2000
1600
1200
800
400
0
0 5 10 15 20 25
Rings
0
2.75
4.75
13
24
35
59
251.5

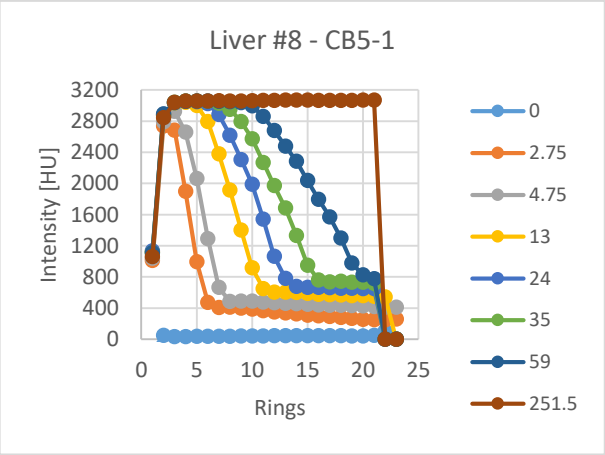
Liver #8 - CB5-1
Intensity [HU]
3200
2800
2400
2000
1600
1200
800
400
0
0 5 10 15 20 25
Rings
0
2.75
4.75
13
24
35
59
251.5

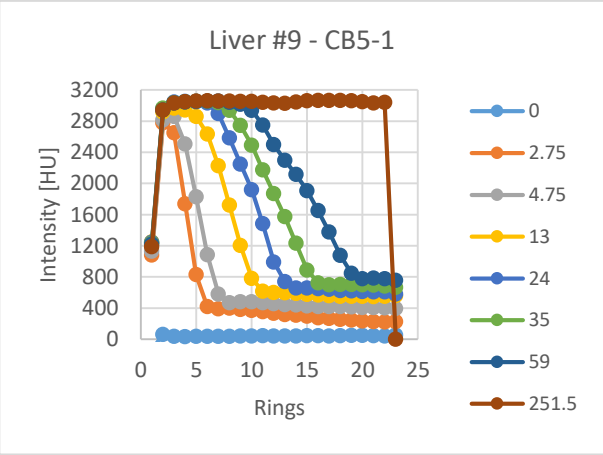
Liver #9 - CB5-1
Intensity [HU]
3200
2800
2400
2000
1600
1200
800
400
0
0 5 10 15 20 25
Rings
0
2.75
4.75
13
24
35
59
251.5

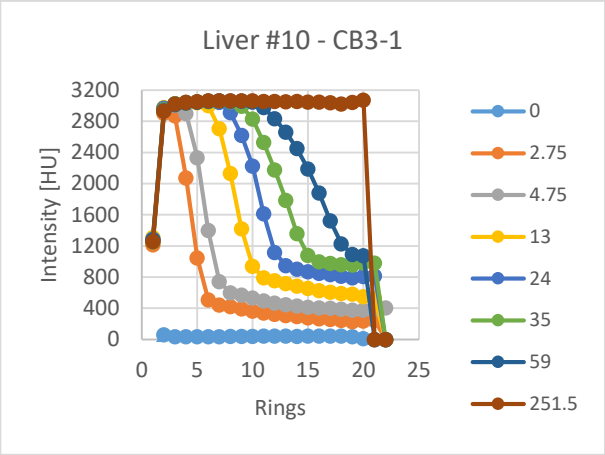
Liver #10 - CB3-1
Intensity [HU]
3200
2800
2400
2000
1600
1200
800
400
0
0 5 10 15 20 25
Rings
0
2.75
4.75
13
24
35
59
251.5

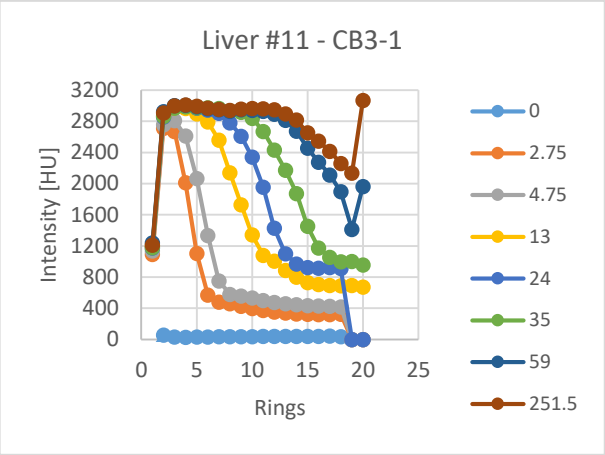
Liver #11 - CB3-1
Intensity [HU]
3200
2800
2400
2000
1600
1200
800
400
0
0 5 10 15 20 25
Rings
0
2.75
4.75
13
24
35
59
251.5

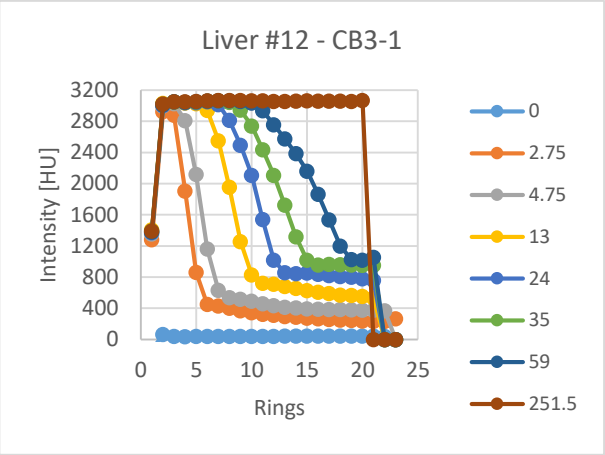
Liver #12 - CB3-1
Intensity [HU]
3200
2800
2400
2000
1600
1200
800
400
0
0 5 10 15 20 25
Rings
0
2.75
4.75
13
24
35
59
251.5

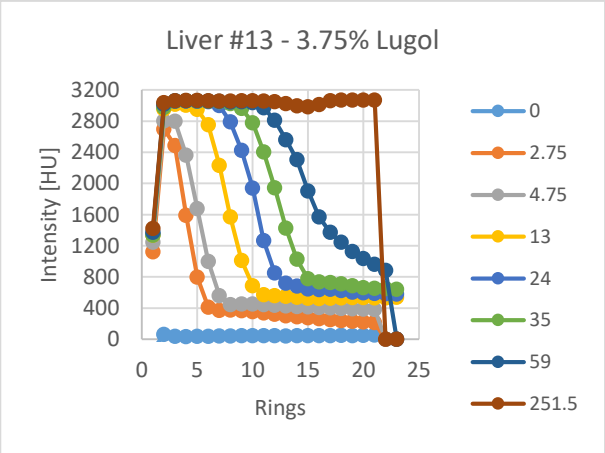
Liver #13 - 3.75% Lugol
Intensity [HU]
3200
2800
2400
2000
1600
1200
800
400
0
0 5 10 15 20 25
Rings
0
2.75
4.75
13
24
35
59
251.5

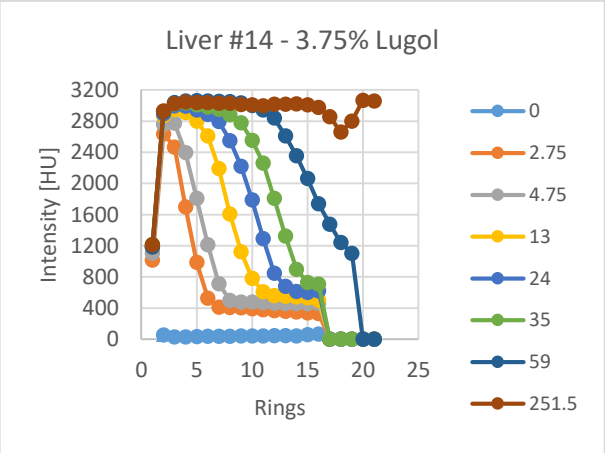
Liver #14 - 3.75% Lugol
Intensity [HU]
3200
2800
2400
2000
1600
1200
800
400
0
0 5 10 15 20 25
Rings
0
2.75
4.75
13
24
35
59
251.5

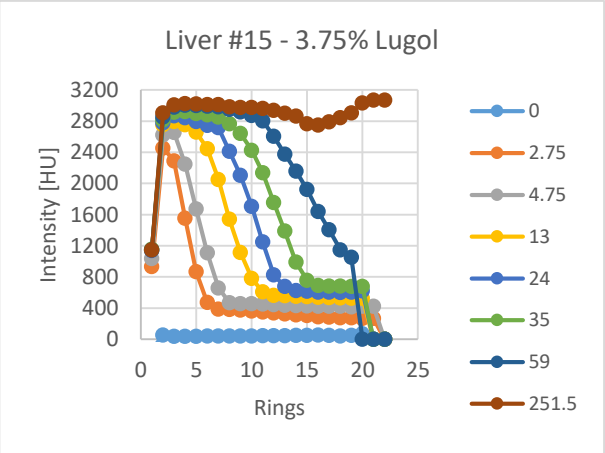
Liver #15 - 3.75% Lugol
Intensity [HU]
3200
2800
2400
2000
1600
1200
800
400
0
0 5 10 15 20 25
Rings
0
2.75
4.75
13
24
35
59
251.5

Appendix VII – Arthurs Method

Pork Liver Samples

This appendix contains a description of the solutions used during the Arthurs method tests.
15 Pork liver samples were immersed in:

1. Lugol Formalin (LF)-solution (n = 3)
   15% Lugol's solution (5 gr. I_2 + 10 gr. KI + 100 mL Milli-Q water) + 10% w/v formalin = 7.5% LF-solution
2. Formalin Buffered Lugol (FBL)-solution (n = 3)
   15% 2x Sörensen's Buffered-Lugol + 10% w/v formalin = 7.5% FBL-solution
3. Formalin (F)-solution (n = 3)
   10% w/v formalin
4. Formalin Buffered (FB)-solution (n = 3)
   2x Sörensen's Buffer (at pH = 7) + 10% w/v formalin = 1x FB
5. 7.5% Lugol's (L)-solution (n = 3)
   5 gr. I_2 + 10 gr. KI + 200 mL Milli-Q water

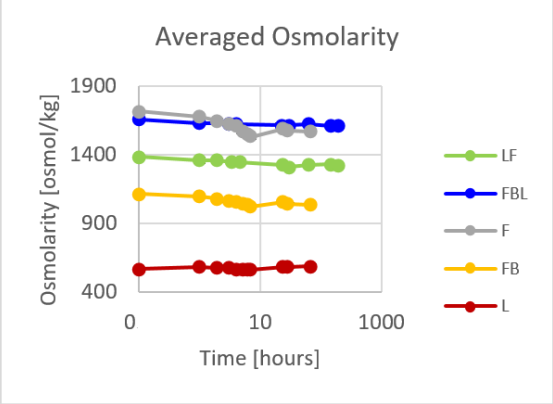

Figure 32 *Averaged osmolarity over time (n = 3) of fresh pork liver samples.*

Liver weights were approximately between 1.1 and 1.7 grams. Amount of solution used was therefore between 11 and 17 mL (approximately 10x tissue weight).

Foetuses

In this appendix the weight, osmolarity and optical density measurements results of TOP175 and TOP176 are presented in *Figure 33 – Figure 35*.

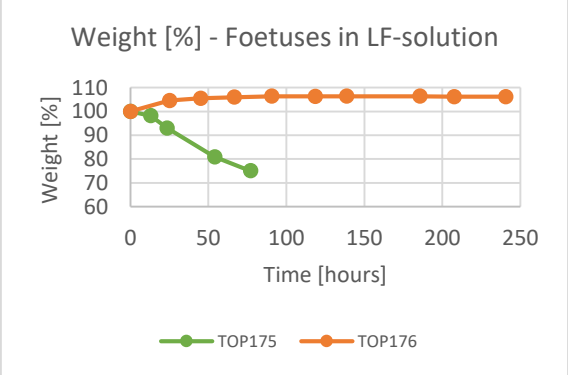

Figure 33 *Weight over time (in percentages) of TOP175 and TOP176 relative to the starting weight.*

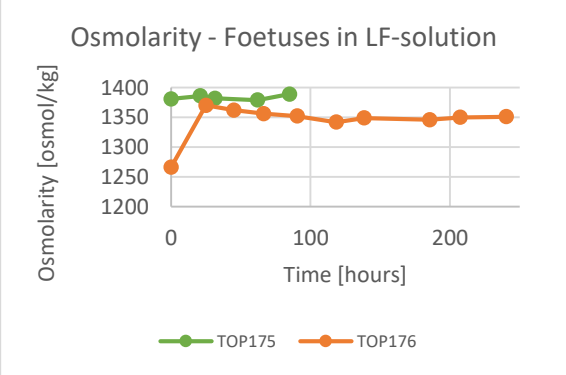

Figure 34 *Osmolarity over time of TOP175 and TOP176.*

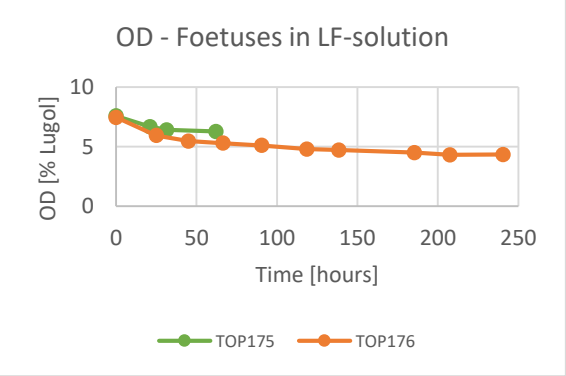

Figure 35 *Optical density over time expressed in percentages Lugol's solution present in the solution.*

Appendix VIII – AMIRA Recipes

This appendix contains an explanation of the recipes used in the software AMIRA (Version 2020.2) to determine the volume- (see *Figure 36*) and distance/intensity measurements (staining progress) (see *Figure 37*) pork liver samples and foetuses. The AMIRA recipes are created by Jaco Hagoort.

Volume Measurements of Pork Liver Samples

Recipe for volume measurements of liver blocks (CT images).
Original data resolution is 0.1 x 0.1 x 0.1 (mm^3), tested and correct for 0.2 mm resolution.

Recipe: Res02_Th750_OR_Th-400erosion1_rem1000_zposvolmeanmedian.hxrecipe
Res02_Th950_OR_Th-400erosion1_rem1000_zposvolmeanmedian.hxrecipe

Based on: Res02_Th-400ORTh750_Measure volume and zpos.hx
Res02_Th-400ORTh950_Measure volume and zpos.hx

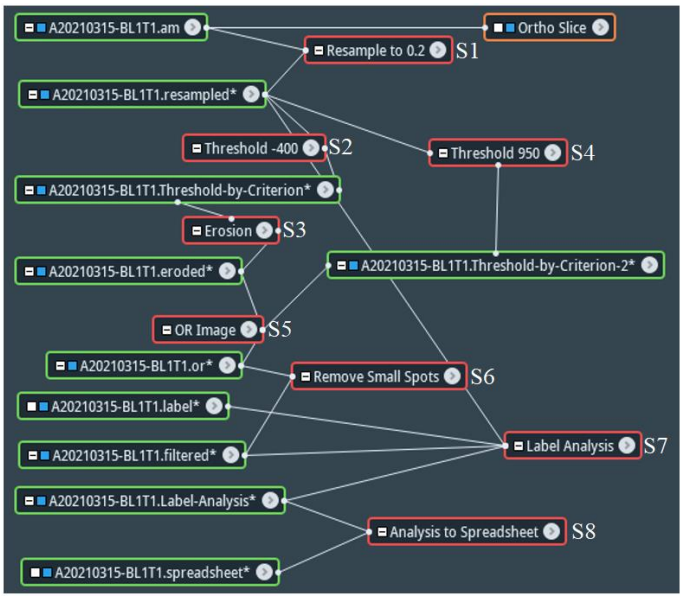

Figure 36 *Project view of the volume measurements in the software AMIRA (Version 2020.2).*

Steps (red boxes in *Figure 36*):

S1 Resample data to isotropic 0.2 mm
Changes the resolution of any 3D regular field.

S2 Threshold greater than -400
Performs thresholding based on a comparison criterion.

S3 Erosion
Removes transition from air to (stained) soft-tissue and ends up with only thresholding the (stained) soft-tissue.

S4 Threshold greater than 750 or 950
Performs thresholding based on a comparison criterion. The comparison criterion in this case is based on a threshold of -400 to 750 for T1 and a threshold from -400 to 950 for T2 (and later timepoints).
The threshold for T1 (-400 to 750) is set due to 750 being in the median of HU_{air} and $HU_{unstained\ soft-tissue}$ (based on 2500 HU or lower). The threshold for T2 (and later timepoints) (-400 to 950) is set due to 950 being the median of HU_{air} and $HU_{stained\ soft-tissue}$ (based on 3000 HU or higher).

S5 OR Image
Performs a logical OR between two images.

S6 Remove Small Spots (3D) < 1000 voxels

S7 Label Analysis (3D, basic):
Creates a labelfile with 1 material per block
To get 1 labelfile with volume values per block

S8 Analysis to Spreadsheet
Label Analysis (3D, Zpos, Mean), Analysis to spreadsheet. Measurement output in the form of a table.
Spreadsheet contains: BaryCenterZ, Volume3D [mL], Mean [HU], Median [HU] and index number.

Distance/Intensity Measurements (Staining Progress) of Pork Liver Samples
Recipe for distance measurements of liver blocks (CT images).
Recipe: Res02_Th-400_Fill1000_split_Distancemap_matx100.hxrecipe
Based on: T1am_Res02_Th-400_Fill1000_split_Distancemap_matx100.hx

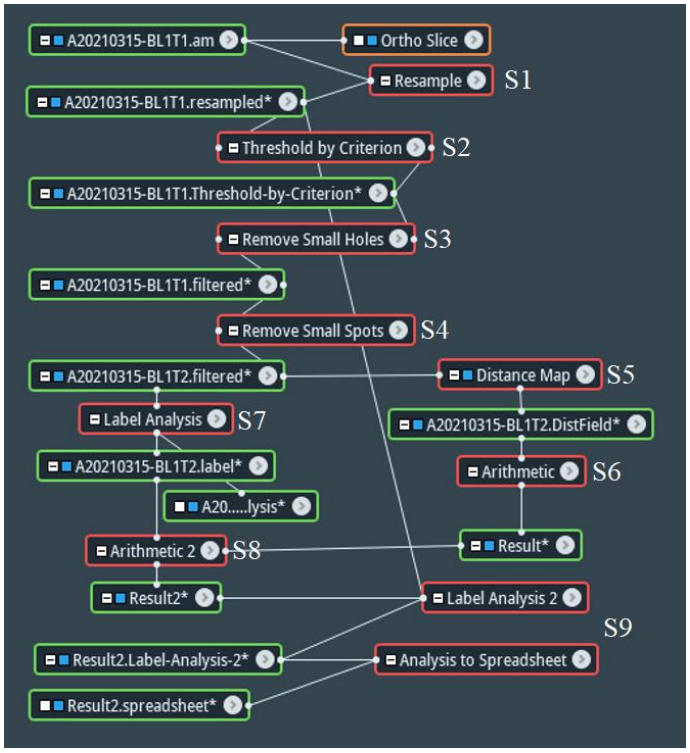

Figure 37 *Project view of the distance/intensity measurements (staining progress) in the software AMIRA (Version 2020.2).*

Created for one column of blocks. Block 1 should be at the "feet" position (lowest z-position value).
Original data resolution is 0.1 x 0.1 x 0.1 (mm^3), tested and correct for 0.2 mm resolution.
Distance per ring is $\frac{1\ mm}{4} = 0.25\ mm$ (See S6).

Steps (red boxes in *Figure 37*):
S1 Resample data to isotropic 0.2 mm
Changes the resolution of any 3D regular field.

S2 Threshold greater than -400
Performs thresholding based on a comparison criterion.

S3 Remove small holes (3D) < 1000 voxels (= Fill Holes)

S4 Remove small spots (3D) < 1000 voxels

S5 Distancemap (Champfer, float, inside): result values 0…6.1 (= 6.1 mm)
Computes a 3D distance field from a binary image.

To get more and smaller discrete steps in a 8-bit label file:
S6 Arithmetic(A*4)+1 : result values 1…25.6

Creates a labelfile with 1 material per block
S7 (Data = S4) Label Analysis (3D, basic):

To get 1 labelfile with ringvalues per block
S8 (A=S7, B= S6) Arithmetic (100*A+B): result
Label 1..100 = Exterior (=1)
Label 101..200 = Ring 1..100 of block 1
Label 201..300 = Ring 1..100 of block 2
..
Label 1500..1599 = Ring 1..100 of block 15

Measure mean grey value per ring per block
S9 (Data = S8, Intensity = S1) Label Analysis (3D, Zpos, Mean), Analysis to spreadsheet.
Measurement output in the form of a table.

Volume Measurements & Distance/Intensity Measurements (Staining Progress) of Foetuses

Regarding the foetuses, a two steps were performed to calculate the volumes. First, a manual segmentation is performed with thresholding at -500, 0 or 500. Thresholding corrections were made with the “Paint Brush” option. Secondly, a watershed segmentation is performed based on the manual segmentation. Via the watershed segmentation, a build-in function in AMIRA, different objects in an image can be separated using an algorithm. Thereafter, the staining progress was objectively assessed by visual inspection.